Consciousness and Cognition 135 (2025) 103935

Contents lists available at ScienceDirect

Consciousness and Cognition

journal homepage: www.elsevier.com/locate/yccog

Full Length Article

ERP responses reveal different neural mechanisms for perception of electrical and tactile stimuli

Jona Förster [a,b,*], Giovanni Vardiero [a], Till Nierhaus [a], Felix Blankenburg [a,b]

[a] Neurocomputation and Neuroimaging Unit, Freie Universität Berlin 14195 Berlin, Germany
[b] Berlin School of Mind and Brain, Humboldt-Universität Zu Berlin 10117 Berlin, Germany

ARTICLE INFO

Keywords:
Electrical stimulation
Mechanical stimulation
Somatosensory awareness
EEG
Single-trial modelling
Bayesian model selection

ABSTRACT

EEG studies have identified ERP components at various latencies as predictors of conscious somatosensory perception, but it remains largely unclear which factors are responsible for this variation. Here, for the first time we directly compare the event-related potential correlates of stimulus detection under tactile versus electrical *peri*-threshold stimulation using single-trial modelling and Bayesian model selection within and between groups, while controlling for task-relevance and post-perceptual processes with a visual-somatosensory matching task. We find evidence that the P50 component predicts conscious perception under tactile, but not electrical stimulation: while electrical stimulation evokes a P50 already for subliminal stimuli and activity in this time window is best explained by stimulus intensity, there is almost no subliminal P50 for tactile stimulation, and detection best explains the data. In contrast, the N80 and N140 components correlate with detection and detection probability in both stimulation groups. The P100 and the P300 were modulated by detection in the tactile group, and by detection probability in the electrical group. Our results indicate that cortical processing in somatosensory target detection partly depends on the type of stimulation used. We propose that electrical stimulation of afferent nerve fibers that do not give rise to conscious perception may mask the P50 modulation associated with conscious somatosensory detection, and might contribute to subliminal evoked cortical responses.

1. Introduction

Long before the seminal paper by Crick and Koch (1990) sparked the modern study of neural correlates of consciousness (NCCs), electrophysiological research on conscious perception in the somatosensory domain had already debated whether early evoked potentials might constitute candidates for somatosensory NCCs. Benjamin Libet's finding that peripheral stimulation at intensities below the threshold of detection elicited subdurally recordable responses in primary somatosensory cortex (SI) suggested that the earliest SI activity is not sufficient for conscious perception (Libet, 1993; Libet et al., 1967). This result has later been replicated (Ray et al., 1999), and more recent studies have confirmed the existence of subthreshold potentials recordable even from the scalp (Forschack et al., 2017, 2020; Nierhaus et al., 2015). Both sub- and supraliminally, the amplitude of early event-related potential (ERP) components has often been found to covary with physical stimulus parameters. In particular, the P50 has been shown to increase linearly with stimulus intensity (Forschack et al., 2020; Nierhaus et al., 2015; Schröder et al., 2021). The P50 and its magnetoencephalographic (MEG)

* Corresponding author at: FU Berlin, Habelschwerdter Allee 45, 14195 Berlin, Germany.
E-mail address: jona.foerster@fu-berlin.de (J. Förster).

https://doi.org/10.1016/j.concog.2025.103935
Received 24 June 2025; Received in revised form 15 September 2025; Accepted 15 September 2025
Available online 27 September 2025

analogue have consistently been shown to originate in SI, with areas 1 and 3b as main contributors (Allison et al., 1992; Jones et al., 2007). In contrast, it has been shown that conscious experience is better tracked by later potentials in NCC studies using somatosensory threshold detection (Auksztulewicz et al., 2012; Forschack et al., 2020; Nierhaus et al., 2015; Schröder et al., 2021; Zhang & Ding, 2009) or masking paradigms (Schubert et al., 2006). An effect of conscious perception on the N80 component has sometimes (Auksztulewicz et al., 2012; Auksztulewicz & Blankenburg, 2013), but not always (Schröder et al., 2021; Schubert et al., 2006) been found in studies applying electrical stimulation. Using mechanical finger stimulation in threshold detection tasks, Jones et al. (2007) found an effect of detection in the M70 event-related field (ERF) component, while Soininen and Järvilehto (1983), mechanically stimulating the hairy skin on the back of the hand, reported no corresponding effect. Furthermore, both with electrical (Ai & Ro, 2013; Schubert et al., 2006) and mechanical (Soininen & Järvilehto, 1983) stimulation, the P100, which involves SI (Allison et al., 1992) but most likely further sources such as bilateral secondary somatosensory cortex (SII) and posterior parietal cortex as well (Forss et al., 1994; Forss, Salmelin, et al., 1994; Mauguière et al., 1997), is sometimes predictive of perception, but this is not always the case (Schröder et al., 2021). Most consistently reported, the N140, with likely origins in bilateral SII (Auksztulewicz et al., 2012; Auksztulewicz & Blankenburg, 2013; Frot & Mauguière, 2003) and possibly frontal contributions (Allison et al., 1992) is well established as a somatosensory NCC in electrical studies (Ai & Ro, 2013; Auksztulewicz et al., 2012; Forschack et al., 2020; Schröder et al., 2021; Schubert et al., 2006; Zhang & Ding, 2009); the tactile EEG study by Soininen and Järvilehto (1983) found a comparable N190 component, and the tactile MEG study by Jones et al. (2007) identified an M135 response. Finally, the P300 (P400 in Soininen and Järvilehto, 1983) amplitude is higher for detected than for undetected stimuli, but in a recent study this effect vanished when post-perceptual processes were controlled for (Schröder et al., 2021).

However, while the P50 partly reflects initial sensory processing, top-down attentional influences on the P50 (or P40) have been reported as well both in the sub- (Forschack et al., 2017) and in the supra-threshold case (Desmedt et al., 1983; Desmedt & Tomberg, 1989; Josiassen et al., 1990), and invasive studies in awake rhesus monkeys found that the amplitude of an N1 potential around 50 ms post-stimulus varies with stimulus detection (Cauller & Kulics, 1991; Kulics, 1982). This component was proposed to correspond to the scalp-recorded N60 component in humans, likewise thought to originate from area 1 of SI (Allison et al., 1992). Moreover, early human surgery (Hensel & Boman, 1960) and later human microneurographic studies (Johansson & Vallbo, 1979; Vallbo & Johansson, 1984) suggested that a single impulse to only one or a handful of peripheral mechanoreceptors may be sufficient to induce subjective detection of that impulse, and in rats, weak microstimulation of a single pyramidal neuron in barrel cortex suffices to elicit detection report behavior (Houweling & Brecht, 2008). In humans, Soininen and Järvilehto (1983) found that the detection of mechanical stimuli delivered to the back of the left hand at subjective threshold intensity evoked a P50 component that was absent for undetected stimuli of the same intensity. Some more recent studies have likewise found early ERP or ERF differences for detected vs. undetected stimuli, at 70 ms (Hirvonen & Palva, 2016; Jones et al., 2007) or even 30 ms post-stimulus (Palva et al., 2005).

In sum, EEG potentials in the P50 time range were found not to be predictive of perceptual experience by most, but not by all studies of conscious somatosensory detection. This raises the question what might be responsible for these divergent findings. While the above-cited studies also vary in the stimulation intensities and sites, as well as different tasks used, one obvious contender for the difference-maker is the type of stimulation: whereas most studies employed electrical stimulation (usually of the median nerve at the wrist or of one or more fingers), only a small minority used mechanical tactile stimulation. And while among the studies that report early ERP/ERF differences between detected and undetected stimuli some used electrical (Hirvonen & Palva, 2016; Palva et al., 2005) and some tactile stimulation (Jones et al., 2007; Soininen & Järvilehto, 1983), the studies that reported no connection between early potential amplitudes and conscious detection invariably used electrical stimulation (Auksztulewicz et al., 2012; Forschack et al., 2020; Libet et al., 1967; Ray et al., 1999; Schröder et al., 2021; Schubert et al., 2006; Uemura et al., 2021; Zhang & Ding, 2009). This might be due to the fact that electrical stimulation constitutes an artificial type of stimulation rarely experienced outside the experimental context, and may consequently engage distinct processing mechanisms (Alouit et al., 2025). Indeed, studies of consciousness that attempted to increase the ecological validity of the employed stimuli or task have sometimes found different or stronger effects (Mudrik et al., 2024). Thus, there is the intriguing, as yet unexplored possibility that the NCCs of somatosensory detection might differ for tactile compared to electrical stimuli. While there are several somatosensory ERP studies comparing different stimulation types for strong supra-threshold stimuli (e.g., mechanical fingernail stimulation versus electrical stimulation: Pratt et al., 1979; pin pricks and taps versus electrical stimulation: Yamauchi et al., 1981; air-puffs versus electrical stimulation: Forss et al., 1994; Rossini et al., 1996), to our knowledge no study so far systematically compared the difference in early ERPs between detected and undetected *peri*-threshold stimuli for tactile versus electrical stimulus types. Alouit et al. (2025) have made an important advance by comparing electrical and vibrotactile stimulation at various frequencies in different fingers, and have found lower component latencies in response to electrical stimulation, as well as different functional connectivity profiles and source reconstructions for the two stimulation types. These results suggest spatiotemporally different cortical processing for electrical and tactile stimulation; however, as the stimulation was supra-threshold, the question of whether and how these stimulation types influence the difference between conscious and unconscious processing remains open. Given that the widely held view that the P50 can be evoked subliminally and largely reflects exogenous factors was achieved using electrical stimulation (Forschack et al., 2020; Libet et al., 1967; Nierhaus et al., 2015; Ray et al., 1999; Schröder et al., 2021), it is particularly interesting to investigate the effect of different stimulation types on early cortical processing of sub- versus supraliminal stimulation.

Therefore, in this study we use single-trial modelling of EEG data in combination with Bayesian model comparison to examine the effects of mechanical versus electrical stimulation of the left index finger at various sub- and suprathreshold intensities in an otherwise identical paradigm, using considerably larger sample sizes than the previous mechanical stimulation studies (Jones et al., 2007; Soininen & Järvilehto, 1983). At the same time, we control for possible effects of task-relevance and associated post-perceptual processes such as perceptual decision-making by means of a visual-somatosensory matching task. This is crucial, as without such control, later occurring ERP components can be mistaken for NCCs when they instead reflect differences in task-relevance or response preparation (Förster et al., 2020; Pitts et al., 2014; Schröder et al., 2021). Our aim in this study was to investigate whether cortical processing across the post-stimulus interval, with a focus on the P50, was best explained by physical stimulus intensity, subjective perception (hit versus miss), or other features of our experimental design, both within and between the two groups (tactile versus electrical).

2. Methods and materials

2.1. Participants

Participants were recruited among the students of Freie Universität Berlin. All participants gave their written informed consent and declared to have no physical or psychological illness, and to be right-handed according to the Edinburgh Handedness Inventory (Oldfield, 1971). Participants first had to perform a behavioral training session in order to ensure that they had stable psychometric functions and sufficient task performance to be included in the main experiment, which took place on a separate day. Twenty-nine participants completed the mechanical stimulation experiment (tactile group). Of these, four participants were excluded due to poor psychometric functions in the main experiment, resulting in twenty-five participants (14 female, 11 male, age range 19–32 years) that were included in the analyses. The electrical stimulation experiment was completed by twenty-eight participants (electrical group), of which three were excluded for the same reason as in the tactile group, again resulting in twenty-five participants (16 female, 9 male, age range 21–35 years). Participants received compensation in the form of either money or course credits. The study was approved by the local ethics committee of the Freie Universität Berlin (003/2021) and conducted in accordance with the Declaration of Helsinki.

2.2. Experimental design

Participants performed a two-alternative forced-choice detection task via a visual-somatosensory matching task (Fig. 1) that has already been employed in several previous studies (Förster et al., 2025; Schröder et al., 2019, 2021). Participants were seated in front of a computer screen and their eye movements were recorded with an eye tracker (SMI RED-m remote, 120 Hz, Sensomotoric Instruments, Teltow, Germany). Every trial started with the appearance of a medium brightness gray fixation disk at the center of a black background. Participants were then presented with either mechanical (tactile group) or electrical (electrical group) stimuli, delivered

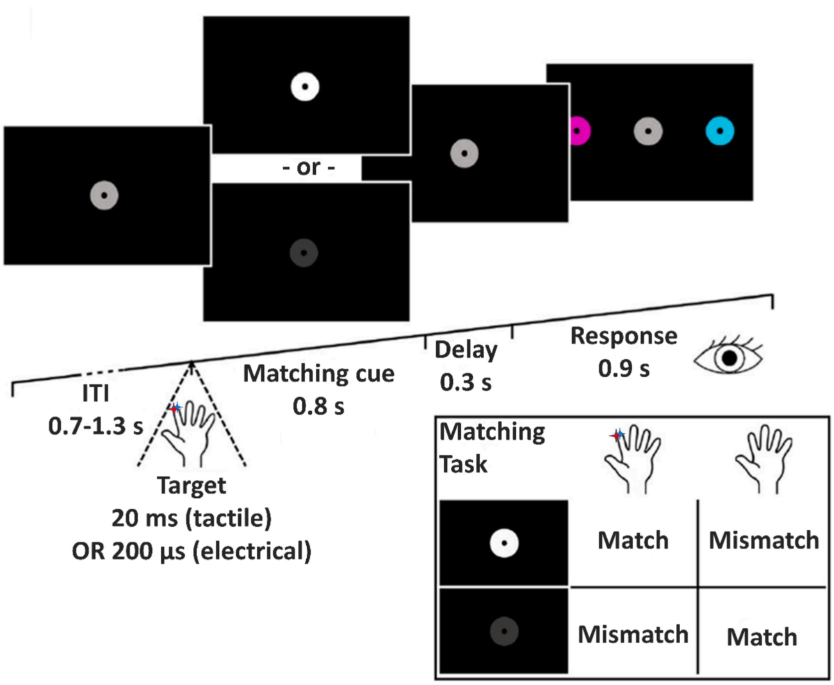

Fig. 1. Experimental Design. After a jittered ITI, participants received a mechanical impulse (tactile group) or an electrical pulse (electrical group) to the pulp of the distal phalange of their left index finger at 1 of 10 individually calibrated intensities on each trial. Simultaneously, the gray fixation disk turned into a visual matching cue by changing its brightness, signaling either target presence (white) or target absence (dark gray). Participants then compared their percept (detected vs. not detected) to the visual cue and decided whether their somatosensory experience matched the meaning of the cue (according to the box on the lower right side of the Fig.). Following a brief delay, participants reported their decision by saccading to one of two color-coded response cues presented at the sides of the screen.

at 1 of 10 different intensities to their left fingertip. The intensities were chosen to sample the entire individual psychometric function, which served to maintain participants' attention and interest in the task and prevent them from mere guessing, and enabled us to identify slight shifts of the detection threshold over the course of the experiment and to monitor task performance. Simultaneous to the onset of stimulation, a visual matching cue was presented for 800 ms. The matching cue consisted of a change in brightness of the gray fixation disk to either white or dark gray, signifying target presence or absence, respectively. After each stimulus presentation, the fixation disk returned to medium brightness for 300 ms, and two colored disks appeared for 900 ms on the left and right sides on the screen (counterbalanced across trials). The colors coded for "match" and "mismatch" (counterbalanced across participants), and participants responded by directing their gaze to the disk that corresponded to their experience (match or mismatch of somatosensory experience and visual cue). This match-mismatch procedure served to decorrelate somatosensory target detection from overt reports, while using saccades instead of button presses to respond ensured that stimulus-evoked electrophysiological activity recorded from somatosensory regions could not be contaminated by response-related activity from the hand region of the adjacent motor cortex. When participants gave their response in time, the chosen response cue briefly increased in size; when they were too slow (>0.9 s), the gray fixation disk in the center of the screen briefly turned red, signaling a missed trial. Individual trials were separated by intertrial intervals (ITIs) randomly jittered between 0.7 and 1.3 s (uniform distribution).

2.3. Stimuli

The mechanical stimuli were impulses with 20 ms duration (the shortest time that would yield stable psychometric functions when piloting the study) that were delivered to the pulp of the left index finger's distal phalange using a single pin of a piezoelectric Braille display controlled by a programmable stimulator (Piezostimulator, QuaeroSys, St. Johann, Germany). The Braille module was taped to the finger firmly enough to prevent the pin position from changing, but gently enough not to cause blood flow sensations that might be confused with the mechanical stimulation. Participants in the tactile group wore earplugs to prevent auditory perception of the pin motion. Stimulus intensity was controlled via the pin's protrusion (0–1.5 mm, controlled in arbitrary units [a.u.] of 0–4096). The electrical stimuli were direct current square wave pulses of 0.2 ms duration (a time commonly used in comparable studies, cf. Auksztulewicz et al., 2012; Auksztulewicz & Blankenburg, 2013; Schröder et al., 2021), delivered via adhesive electrodes (GVB-geliMED, Bad Segeberg, Germany) at the same location using a DS5 constant current generator (Digitimer Limited, Welwyn Garden City, Hertfordshire, UK). The stimulation site was indicated to each participant as exactly as possible by indenting it with the tip of a pen. Then, the position of the stimulation device (the Braille module in the tactile, and the adhesive electrodes in the electrical case) was adjusted until the participant reported that the stimulation site coincided with the previously indicated site. The arm and stimulated hand rested loosely on the table with the palm facing downward, and participants were instructed to move them as little as possible during the experiment. In both groups, we began by determining participants' individual detection threshold by a brief staircase procedure: starting from an initial intensity value (tactile: 800 a.u., electrical: 0.5 mA), this value was increased by 100 a.u. (tactile) or 0.1 mA (electrical) until the participant reported to feel the pulse. The stepsize was then halved, and the intensity decreased by the new stepsize until the participant reported not feeling the pulse anymore. The stepsize was then again halved, and the intensity increased by the new stepsize, and so on for three up- and three down-progressions in total. Starting from these values, participants' psychometric functions were estimated in order to accommodate between-subject variation in detection thresholds and criteria. Participants received 15 intensities (20 repetitions per intensity, leading to 300 trials in total), linearly spaced around their initial detection threshold. After each stimulus presentation, they were required to respond via keyboard whether they had detected the pulse. A logistic function with two parameters (detection threshold and slope at threshold) was then fitted to the data (estimated 1 %, 50 %, and 99 % detection thresholds: $T01 = 534 \pm 159$ a.u., $T50 = 834 \pm 118$ a.u., $T99 = 1134 \pm 223$ a.u. in the tactile group, and $T01 = 1.09 \pm 0.4$ mA, $T50 = 1.46 \pm 0.42$ mA, $T99 = 1.82 \pm 0.52$ mA in the electrical group; all descriptive statistics are reported as mean $\pm$ SD, except when otherwise noted). Based on these parameters, 10 different equally spaced intensity levels were determined and used in the main experiment. In line with previous studies (Schröder et al., 2019, 2021), the trial numbers within each intensity level followed a normal distribution, such that most trials occurred with an intensity close to the individual detection threshold (intensity levels 5 and 6: 32 trials/run each), and relatively few trials with intensities far from threshold (intensity levels 1 and 10: 8 trials/run each). Stimuli were presented in MATLAB 2013a (The MathWorks, RRID:SCR_001622) via the Psychophysics toolbox (Brainard, 1997).

2.4. Experimental procedure and EEG recording

All participants performed a behavioral training session prior to the experiment and on a separate day to ensure that they had stable psychometric functions, and were invited to the EEG recording only if they reached at least 90 % accuracy in a training run with only sub- and suprathreshold stimulation, demonstrating comprehension of the task and ability to perform it correctly at low error rate. EEG data were recorded from 64 active electrodes positioned according to the extended 10–20 system (ActiveTwo, BioSemi, Amsterdam, Netherlands) with 2048 Hz sampling frequency. Vertical (vEOG) and horizontal (hEOG) eye movements were recorded with four additional electrodes. In the tactile group, eleven participants completed seven runs of 200 trials each (~10 min per run), resulting in a total number of 1400 trials per participant. The remaining fourteen participants in the tactile group completed only six runs (1200 trials), due to fatigue in one or more runs. In the electrical group, twenty participants completed seven runs, and five participants completed only six runs. After the main experiment, a localizer run with suprathreshold stimulation at 2 Hz frequency (jittered with ±10 ms, uniform distribution) was recorded (tactile group: 800 trials, electrical group: 600 trials) to enable delay correction (see below). The intensity was set to be several times above detection threshold, but below motor threshold (tactile group: 4000 a.u., electrical group: 4.05 mA ± 0.77 mA).

2.5. Data analysis

Behavior. To visualize the distribution of detection thresholds across participants, we fitted logistic functions to the behavioral data of each run and averaged the estimated slope and normalized threshold parameters for each participant, resulting in one mean psychometric function per participant (Fig. 2). Estimated detection probabilities <10 % for intensity level 1 and >90 % for intensity level 10 were defined as inclusion criteria to minimize the possibility of incomplete sampling of individuals' psychometric functions (due to shifts in detection thresholds, response criteria, or erroneous reports). Slope differences between the two groups were tested using a Bayesian two-sample t-test equivalent, and reaction time differences between hits and misses within groups using a Bayesian paired-sample t-test equivalent (Krekelberg, 2022); we report Bayes factors in favor of a difference (BF10). To test whether the matching task was successful in dissociating somatosensory target detection (hits vs. misses) from overt reports (match vs. mismatch), we performed Bayesian tests of association (the Bayesian equivalent to a chi-square test; cf. Albert, 1997) for all participants and report Bayes factors in favor of the null hypothesis (BF01). Following the recommendations by Kass and Raftery (1995), we consider $1 \leq BF < 3$ negligible, $3 \leq BF < 20$ positive, $20 \leq BF < 150$ strong, and $150 \leq BF$ very strong evidence.

EEG preprocessing. Preprocessing was performed using SPM12 for EEG (https://www.fil.ion.ucl.ac.uk/spm) and custom MATLAB scripts. The data were high-pass filtered at 0.01 Hz, notch-filtered between 48–52 Hz, down-sampled to 512 Hz, and re-referenced to common average. Eye blinks were removed from the data using adaptive spatial filtering based on individual blink templates computed from the vEOG (Ille et al., 2002). The data were then epoched from −50 to 600 ms relative to stimulation onset. All epochs were visually inspected for artifacts. Bad channels (containing > 20 % bad trials) were interpolated on a run-by-run basis when only specific runs were affected, or completely when all runs were affected (tactile group: 3.4 ± 1.9 channels, electrical group: 4 ± 2 channels interpolated in at least one run). The remaining artifactual trials were removed (tactile group: 11.4 ± 3.3 %, electrical group: 13.4 ± 3.9 %). The data were then low-pass filtered at 40 Hz and baseline-corrected using a baseline from −50 to −5 ms. Because mechanical stimulation using the Quaerosys stimulator is slightly delayed compared to electrical stimulation with the DS5 and different stimulus durations were used in the two groups, we relied on the localizer data to determine the peak latency of the earliest discernible physiological component, identified as the P50 at the CP4 electrode (tactile group: 50.78 ms; electrical group: 42.97 ms), and corrected all EEG data of the tactile group by that delay (7.81 ms).

EEG data analysis. To test the influence of stimulus intensity, conscious detection, and a number of other aspects of our experimental design on the various ERP components in each of the two stimulation groups, we fitted a series of simple Bayesian GLMs to the single-trial data of each participant, and performed a Bayesian model selection (BMS) (Schröder et al., 2021; Stephan et al., 2009) on the group level within each group, as well as between the two groups (Rigoux et al., 2014). Note that our analysis and, accordingly, the description of the methods and results, are partly based on Schröder et al. (2021). GLMs were formulated that each contained an intercept regressor and an independent variable: (1) physical stimulus intensity (linear regressor, levels 1–10); (2) detection probability (sigmoidal regressor, the individual psychometric function); (3) categorical target detection (binary regressor, hit/miss); (4) expected uncertainty (inverse U-shaped regressor, the first derivative of the individual psychometric function); (5) report type (binary

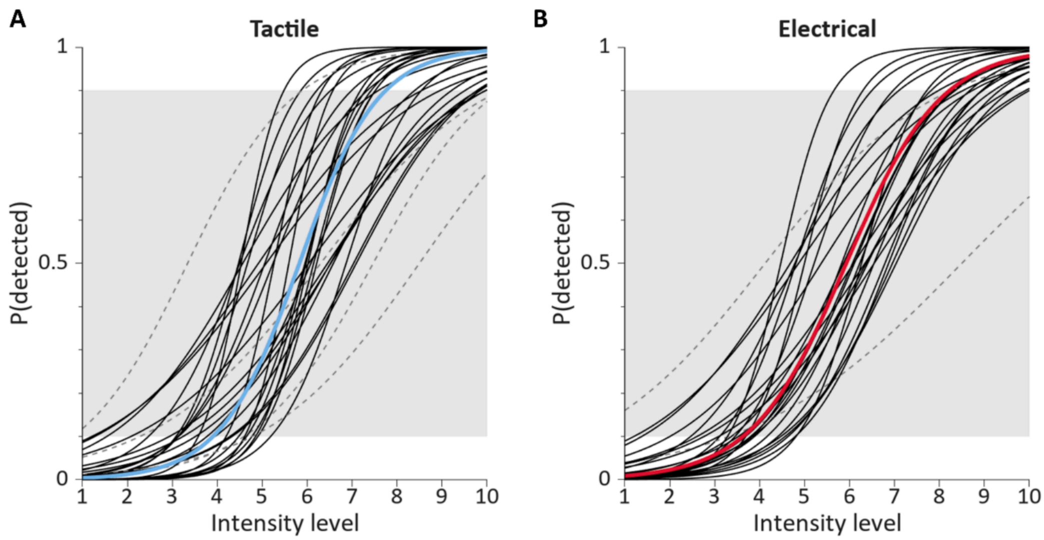

Fig. 2. ***A:*** Normalized mean psychometric function in the tactile group (n = 25). Black lines indicate the individual psychometric functions included in the final sample, averaged over runs and normalized across participants to intensity levels 1–10. Blue thick line denotes the group average. Gray dashed lines indicate participants whose detection probabilities at minimum and maximum intensity levels fell outside the required margin of <10 % and >90 % (white background) and were thus excluded from the analysis. ***B:*** Same as ***A***, but for the electrical group (n = 25). Red thick line denotes the group average.

regressor, match/mismatch); and (6) visual matching cue (binary regressor, white/dark). A seventh (null) model contained only an intercept regressor. To obtain the model evidences required for BMS, we used the Bayesian estimation scheme as implemented in SPM's *spm_vb_glmar.m* function (parameters: AR model order = 0, mean $w0$ = 0, variance α^{-1} = 0.005) to estimate each model, separately for each electrode, time point, and participant. All regressors were z-score-normalized before model fitting to obtain model evidences on the same scale, enabling standardized model comparison. Note that the detection probability model, while different from both the intensity and detection models, comprises features of both these models: like the intensity model, its regressor increases monotonically with stimulus intensity (but unlike the intensity model, it does so in a sigmoidal rather than linear fashion). And like the binary detection model, the detection probability regressor captures an aspect of subjective perception, insofar as the latter model is

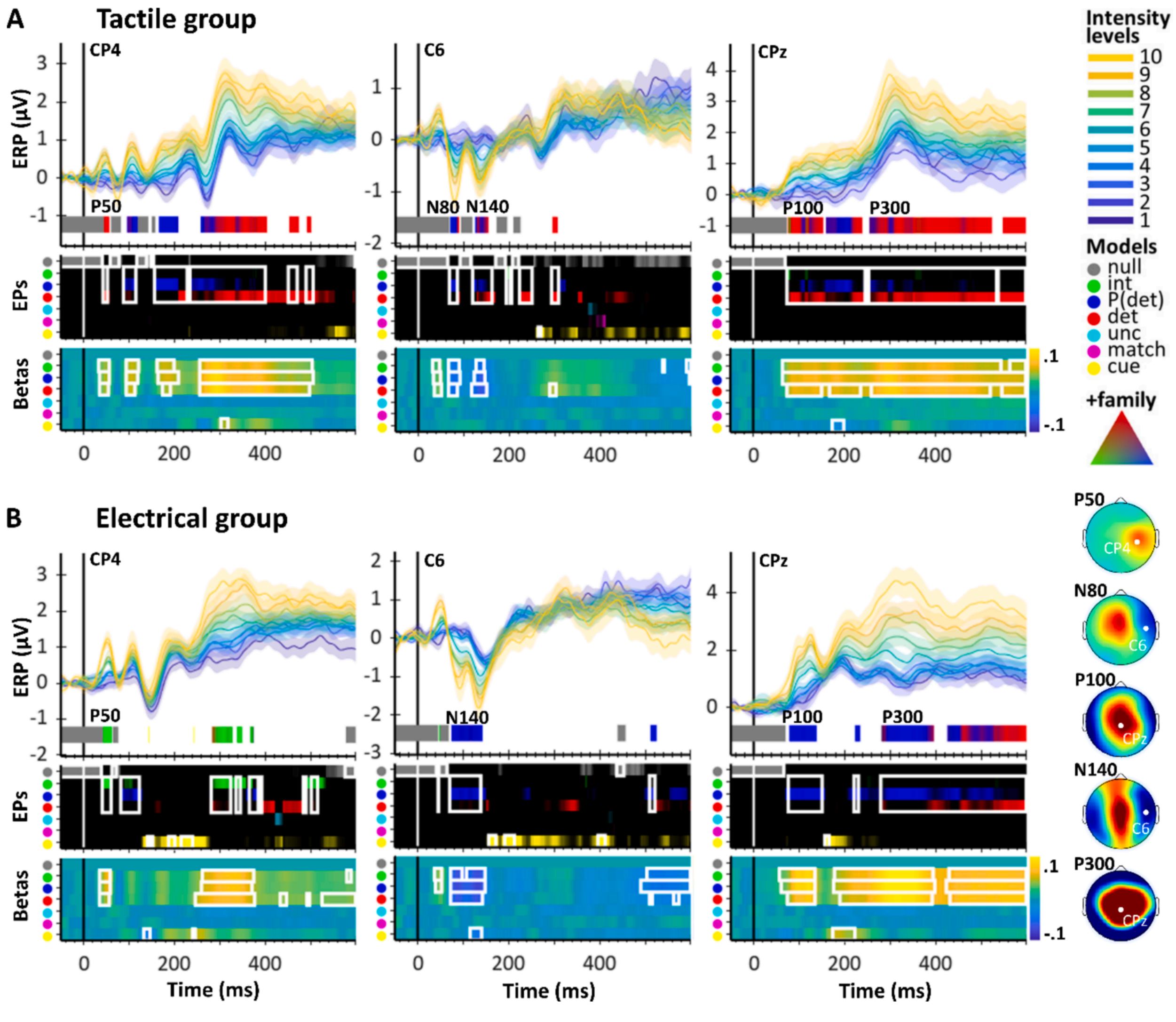

Fig. 3. ***A:*** ERP and BMS results for three electrodes of interest (CP4, C6, CPz, marked in grand-averaged hit topographies on the right) in the tactile group (***A***) and in the electrical group (***B***). For each electrode: Top: Stimulus-locked, grand-averaged ERPs (mean ± SE) for each intensity level (1–10). Below the ERPs, BMS results are plotted for time points of interest (exceedance probability [EP] ≥ 99 % and $BF10_\beta \geq 150$) as color bands representing the winning model families. For time points best modeled by the +family (intensity, detection probability, detection), the color represents an RGB value that is composed of the EPs of the three +family models (compare the RGB triangle: corners correspond to EP = 100 %, signifying a clear winner of the model comparison within the +family, whereas intermixed colors represent similar EPs for the respective models). Middle: Unthresholded EP time courses for each model. Bottom: Time courses of group-averaged β estimates of each model's experimental regressor (warm colors represent positive β estimates; cold colors represent negative β estimates). White rectangles represent data segments that exceed the respective thresholds. The results suggest that the P50 was modulated by detection in the tactile group, whereas it was modulated by stimulus intensity in the electrical group. The P100 was dominated by detection in the tactile group, whereas it was best explained by detection probability in the electrical group. In the tactile group, a clearly separate N80 component showed effects of detection probability transitioning to detection, followed later by the N140 with the same characteristics. In the electrical group, the N80/N140 appeared as one single complex modulated by detection probability. The P300 showed an effect of detection in the tactile group, and an effect of detection probability in the electrical group, transitioning to detection only at even later time points.

derived from the former (namely, it reflects the proportion of detected trials per intensity level). However, unlike the detection model, the regressor has the same value for all trials of a given intensity level, irrespective of whether that trial was a hit or a miss. As such, the detection probability model occupies a middle ground between the intensity and detection models, capturing aspects of both physical and perceptual stimulus processing. Consequently, these three models are partly collinear. This renders classical ERP analysis problematic, because contrasting hits and miss trials (conscious vs. unconscious) would be confounded by the stimulus intensity and/or the detection probability. BMS can address this situation and quantify the degree to which each of a series of collinear models explains variance beyond their shared variance, thereby disentangling the correlated aspects of our experimental design. BMS achieves this by grouping collinear models into model families and adjusting the models' prior probabilities accordingly (Penny et al., 2010). Thus, we combined the correlated intensity, detection, and detection probability models into one family (denoted the +family), and used the VBA toolbox (Daunizeau et al., 2014) to obtain exceedance probabilities (EPs) for each model and time point, quantifying the probability that a given model explains the data better than any of the other models under comparison. A model was designated as

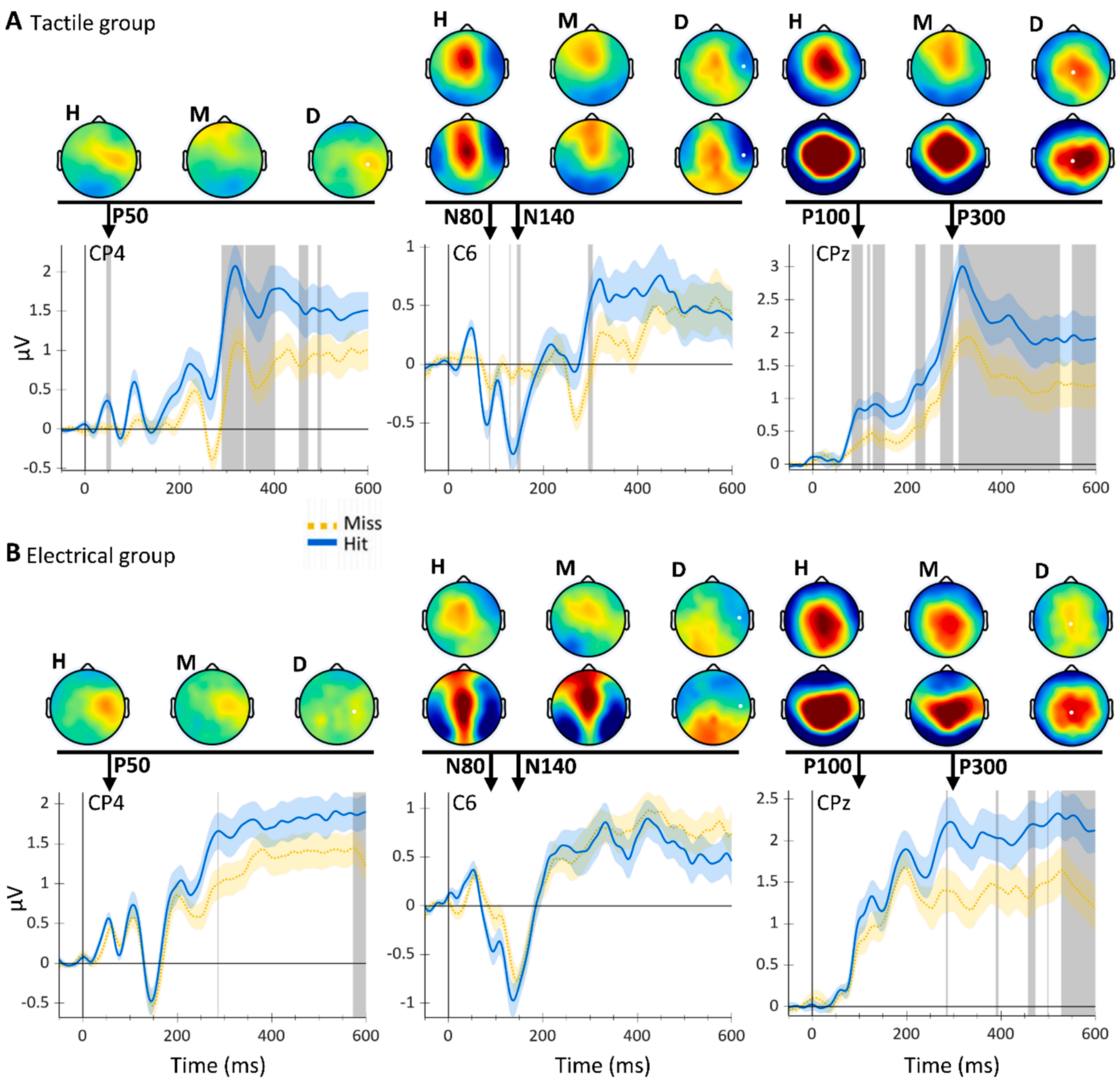

Fig. 4. Intensity-matched hit and miss ERPs (mean ± SE) in (***A***) the tactile group and (***B***) the electrical group. Topographies for hits (H), misses (M), and their difference (D) are displayed for time points of interest (indicated by black arrows). Gray shaded areas represent time points that were best explained by the detection model. The P50 is present for both hits and misses in the electrical group, but absent for misses in the tactile group, corresponding to the BMS results in Fig. 3. The N80 and N140 are weaker for hits than misses in both groups, but much more so in the tactile group. The P300 shows a clear peak at 300 ms for the tactile group, as opposed to a plateau beginning around 200 ms and lasting toward the end of the epoch in the electrical group.

winning at a given time point when it exceeded an EP threshold of 0.99 and the β estimates of the respective regressor deviated systematically (i.e., in the same direction) from zero across participants, as evidenced by a Bayesian one-sample *t*-test equivalent (Krekelberg, 2022) exceeding a β evidence threshold of BF10 $\geq$ 150 (very strong evidence). The null model, lacking an experimental regressor, was only required to meet the first of these criteria (exceeding the EP threshold). Note that an EP threshold of 99 % is analogous to controlling the false discovery rate in classical statistics such that at most 1 % of the data segments exceeding the EP threshold are false positives (Friston & Penny, 2003; Marchini & Presanis, 2004).

Between-groups comparison. To confirm that group-specific results reflect real differences between the two groups, we used VBA's *VBA_groupBMC_btwGroups.m* function (Daunizeau et al., 2014) to quantify the evidence for a between-groups difference in the frequencies with which each model prevailed (Rigoux et al., 2014). Using a hierarchical approach, we first tested whether model frequencies differed between groups on the family level. Next, we tested whether there were between-groups differences within the three models of the +family (intensity, detection, and detection probability). Finally, we tested whether there were between-groups differences in the direct comparison of two +family models of interest at time points where the within-group analysis suggested that (out of these two models) a different model performed best in each group. The between-groups analysis lends strong support to real group differences within +family model frequencies that were observed at the within-group level only when three criteria are fulfilled: (1) at a given time point and electrode, the family-level comparison reveals no evidence for a between-groups difference in model family frequencies (i.e., it is possible that the +family prevailed in both groups); (2) at the same point, there is evidence for a between-groups difference in model frequencies within the +family; and (3) at the same point, there is evidence for a between-groups difference in the frequencies of the two +family models that diverged in the within-group analyses. We report Bayes factors in favor of a difference (BF10).

3. Results

3.1. Behavior

Participants detected 47.77 $\pm$ 9.65 % of the targets in the tactile group and 46.1 $\pm$ 9.08 % in the electrical group. Note that a target was presented on every trial, so that the detection rate was identical to the hit rate, and false alarms and correct rejections could not be defined. As expected by design, experience varied the most on trials with intermediate intensities, leading to sigmoidal psychometric curves (Fig. 2). We found no evidence for a difference in slopes between the two groups (BF10 = 0.95). We found strong evidence for a difference in reaction times between hits and misses in both the tactile (hits: 309.54 $\pm$ 40.46 ms, misses: 317.72 $\pm$ 43.81 ms, BF10 = 197.87) and the electrical group (hits: 316.72 $\pm$ 44.66 ms, misses: 322.59 $\pm$ 44.33 ms, BF10 = 5.24). Bayesian tests of association provided positive evidence that the matching task successfully dissociated target detection from overt reports (3 < BF01 < 10 for all participants in both groups).

3.2. Event-related potentials

To investigate the group-specific effects of the various experimental design aspects encoded in the simple GLMs on our target ERP components, we inspected the BMS results in three electrodes of interest: CP4, C6, and CPz. These electrodes were selected based on Schröder et al. (2021) in order to facilitate direct comparison of the results; grand-averaged signals are plotted for each intensity level in Fig. 3. As confirmed by the grand-averaged topographies of all hit trials across both groups, these electrodes captured the components of interest at relevant time points (Fig. 3). To visualize the effects of detection more directly, we also plotted grand-averaged subsamples of hit and miss trials that were matched for intensity levels (Fig. 4). The P50 in contralateral electrode CP4, the P100 and P300 in electrode CPz, and the N140 in electrode C6 were clearly present in both the tactile and the electrical group. In addition, the tactile group exhibited a clearly separate N80 component, preceding the N140 in the same electrodes, while the same component was much less unambiguously separable from the N140 in the electrical group, where the two components appeared to form a single complex (Figs. 3, 4).

Remarkably, while the P50 amplitude in electrode CP4 was only slightly smaller for misses compared to hits in the electrical group, this component was practically absent for misses in the tactile group (Fig. 4). This observation is reflected in the BMS results: whereas the P50 was best explained by the detection model in the tactile group, it was the intensity model that explained the P50 best in the electrical group (Fig. 3). The N80 and N140 in electrode C6 in the tactile group and the N140 in the electrical group were weaker for misses than hits in both groups, but much more so in the tactile group (Fig. 4). In the tactile group, both the N80 and the N140 were best explained by detection probability in the early part, and by detection in the later part of the components. In the electrical group, the N80/N140 complex was dominated by the detection probability model across its entire duration (Fig. 3). The P100 in electrode CPz had a stronger overall amplitude in the electrical than in the tactile group, but it was stronger for hits than misses in both groups (Fig. 4). In the tactile group, after a brief initial effect of intensity, the P100 was dominated by the detection model, interspersed with brief segments where the detection probability model performed best. In the electrical group, the detection probability model explained the P100 best (Fig. 3). The morphology of the P300 markedly differed between the two groups: the electrically evoked P300 in electrode CPz reached a plateau already around 200 ms, whereas the tactile-evoked P300 began later and peaked sharply at 300 ms before it settled at about the same amplitude as in the electrical group. In both groups, the P300 amplitude was stronger for hits than misses (Fig. 4). In the tactile group, the detection model dominated the P300 across the entire epoch, whereas in the electrical group the P300 was best explained by detection probability for most of the time, transitioning toward detection only toward the end of the epoch (Fig. 3).

3.3. Effects across time and space

To obtain a more comprehensive understanding of the spatiotemporal evolution of model probabilities, we determined the overall model performances across time as defined by the proportion of electrodes showing above-threshold effects for each model (Fig. 5). As expected, neural activity during the baseline interval was most accurately accounted for by the null model. The intensity model did not show large effects in either group. The clearest effect occurred in the electrical group in electrodes CP4 and C4 around ~50 ms, a time range in which no other effects were present anywhere on the scalp, suggesting that physical stimulus intensity alone explained this component. Further effects of stimulus intensity in the electrical group are consistent, but confined to a few central and ipsilateral temporal electrodes, beginning at ~100 ms and reemerging throughout the entire epoch. In the tactile group, the first trace of an intensity effect occurred at ~80 ms, followed by an effect between ~140 ms and ~220 ms. The intensity effect rarely occurs in more than two electrodes simultaneously. The detection and detection probability models play largely complementary roles in the two groups: while both models explain parts of the data in both groups, the detection model strongly outperforms the detection probability model in the tactile group, and vice versa in the electrical group. In the tactile group, the detection model first explains the data in electrode CP4 at ~50 ms, strongly contrasting with the intensity effect in the same electrode and time range in the electrical group. Like in the electrical group, no other effects occur anywhere on the scalp in this time range. Beginning at ~75 ms, detection effects in the tactile group persist throughout the rest of the epoch, first in the N80 time range at contralateral frontal electrodes, followed at ~100 ms by a transient effect in ipsilateral temporal electrodes, as well as a centroparietal effect cluster (corresponding to the P100) that slowly decays until it flares up again in the P300 time range, remaining strong until the end of the epoch. During the N140 time range, detection effects are again visible in contralateral frontocentral and frontal electrodes.

Still in the tactile group, the detection probability model first explains the data in the N80 time range in contralateral frontocentral and -temporal electrodes, before the effect transitions to ipsilateral electrode C5. This pattern is repeated in the N140 time range, when the detection probability effect occurs first in contralateral frontocentral electrodes (now joined by a centroparietal cluster), before shifting toward ipsilateral temporoparietal electrodes around ~150 ms. Beginning at ~300 ms, the detection probability model mostly ceases to explain the signal.

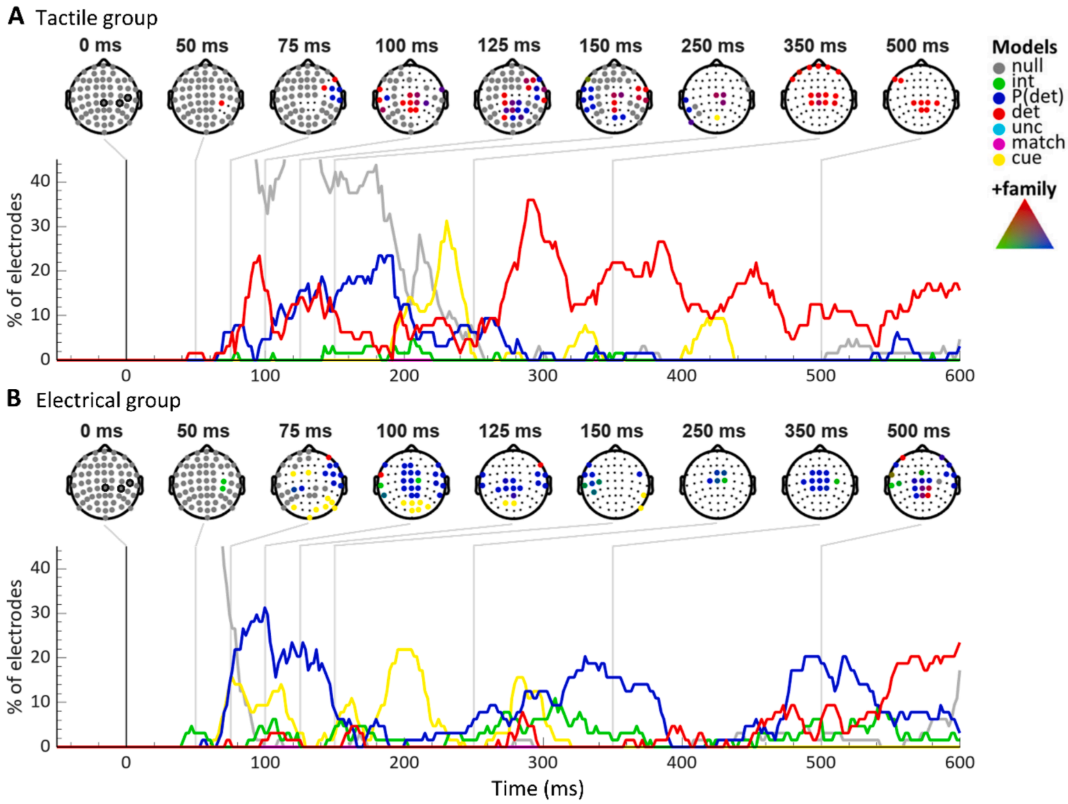

Fig. 5. BMS results across electrodes in the tactile group (***A***) and the electrical group (***B***). For each group, scalp topographies for time points of interest (top) and model time courses across electrodes (bottom) are displayed. The scalp topographies indicate winning models in electrodes surpassing the threshold criteria using colors as in Fig. 3. The circled electrodes at 0 ms represent the electrodes of interest shown in Fig. 3, CP4, C6, and CPz. Model time courses are plotted as the proportion of electrodes showing above-threshold effects over time. The results suggest only minor effects of stimulus intensity in both groups that are almost absent in the tactile group. Overall, in the tactile group the detection model is strongest, whereas the detection probability model dominates in the electrical group.

In stark contrast to the tactile group, detection effects in the electrical group are transient and confined to isolated electrodes, gaining traction only toward the end of the epoch (around ~480 ms) in centroparietal electrodes. However, their spatiotemporal pattern is similar to the tactile group: the first detection effect arises at ~75 ms in contralateral electrode AF8. Like in the tactile group, this effect appears to be the most frontal part of an effect cluster in the N80 time range that is otherwise dominated by the detection probability model, and shifts to ipsilateral electrode FT7 at ~100 ms. This detection/detection probability effect cluster reappears in the N140 time range, with a now slightly more posterior detection effect at ~125 ms in electrode F8. The spatiotemporal evolution of the detection probability model in the electrical group is similar to that of the detection model in the tactile group, with a central cluster beginning at ~100 ms that decays and regains traction around ~200 ms, peaking again in the P300 time range.

Neither the uncertainty nor the report type (match/mismatch) model performed well at any point in either of the two groups, which was not surprising given the identical results by Schröder et al. (2021). The visual matching cue explained the data best in occipital electrodes at various time points, peaking at ~200 ms in both groups.

3.4. Between-groups comparison

To test whether we could reproduce the results obtained within the two groups separately also at the between-groups level (Daunizeau et al., 2014), we inspected whether our electrodes of interest (CP4, C6, CPz) exhibited between-group differences in the relevant model frequencies at the same time points that they showed differences within the groups considered in isolation (Fig. 6). The results confirm that there is no evidence for between-group differences in model frequencies at the family level (BF10 < 3), indicating that models of the +family win at all relevant time points around the ERP components of interest in both groups (first criterion). Furthermore, there are between-group differences between the frequencies of the three +family models in electrode CP4 in the P50 time range and CPz in the P100 and P300 time ranges (BF10 ≥ 3), but not in C6 in the N80 and N140 time ranges (BF10 < 3), confirming the similarities and differences that were observed in the two groups separately, as shown in Fig. 3 (second criterion). Similarly, the frequencies of the detection and intensity models differed between groups in CP4 in the P50 time range, and the frequencies of the detection and detection probability models in CPz in the P100 and P300 time ranges, while these latter model

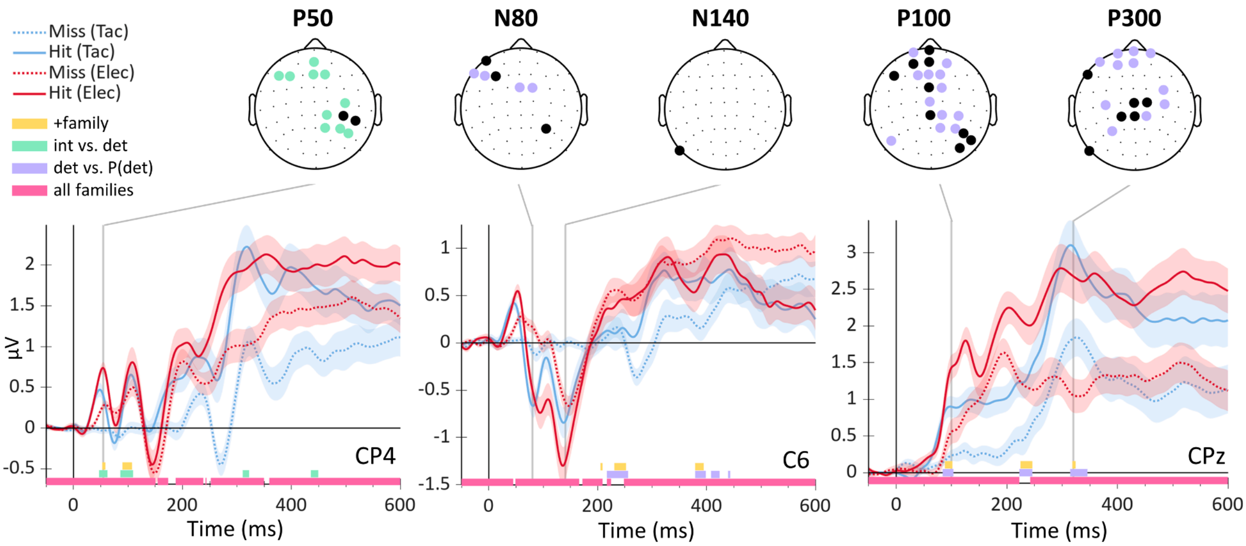

Fig. 6. Between-groups BMS results. The ERP plots show the grand-averaged hit and miss ERPs of the tactile (blue) and electrical (red) groups for the three electrodes of interest (CP4, C6, CPz). The data are the same as in Fig. 3, but plotted by detection (hit/miss) instead of intensity (1–10). The pink color bands at the bottom of the ERP plots represent time points where there was no evidence (BF10 < 3) for a between-groups difference in model frequencies at the level of model families (first criterion). The uppermost, yellow color bands represent time points where there was evidence (BF10 ≥ 3) for a between-groups difference in frequencies of models within the +family (second criterion). For electrode CP4 (left), where the detection model performed best in the tactile and the intensity model performed best in the electrical group in the P50 time range (Fig. 3), the mint-green color band represents evidence (BF10 ≥ 3) that the frequencies of the intensity and detection models differ between the two groups (third criterion). For electrodes C6 and CPz, where all ERP components were best explained by either the detection or the detection probability model in both groups (Fig. 3), the middle, lavender color bands represent evidence (BF10 ≥ 3) that the frequencies of the detection and detection probability models differ between the two groups (third criterion). The topographies (top) show evidence for a between-groups difference in frequencies of the intensity and detection models for the P50 (mint-green), and of the detection and detection probability models for the N80, N140, P100, and P300 (lavender), at time points where all three criteria are met. In electrode C6, the second and third criteria were never met during the N80 and N140 time ranges; here, the topographies are plotted at 80 ms and 140 ms, respectively, to reveal whether electrodes other than C6 differed between groups at these time points. Mint-green and lavender dots represent BF10 ≥ 3, black dots BF10 ≥ 10. The results confirm that the frequencies of the intensity and detection models differ between groups in the relevant contralateral centroparietal electrodes for the P50, and the frequencies of the detection and detection probability models in large frontocentral clusters for the P100 and P300, while the N80 and N140 show no between-group differences in the contralateral frontocentral electrodes that were similar in the two groups (Fig. 5).

frequencies exhibited no group differences in electrode C6 in the N80 and N140 time ranges (third criterion). The topographies plotted at time points where all three criteria are met reveal between-groups differences between the detection and intensity model frequencies in contralateral centroparietal electrodes in the P50 time range, strongest at electrodes CP4 and CP6, as well as wide-spread frontocentral between-groups differences between the detection and detection probability model frequencies, confirming the differences observed at the within-group level (Fig. 5). In the N80 and N140 time ranges, there were no time points in C6 at which all three criteria were simultaneously met; for these ERP components, we plotted topographies at 80 ms and 140 ms, respectively. These topographies exhibit only locally restricted between-groups differences, and no differences at all in the contralateral frontocentral electrodes that also exhibit similarities at the within-group level (Fig. 5). In sum, the results of the between-groups analysis confirm the results observed when considering each group in isolation, and provide evidence for a real difference in model frequencies between the groups.

3.5. Control analysis

To provide additional support for our results, we performed a control analysis at the level of raw voltages (Fig. 7). To minimize the intensity confound, we restricted this analysis to an intensity-matched subsample of trials (as in Fig. 4), and to reduce sampling bias, we drew 40 subsamples per participant (for a total of 1000 subsamples per group) and computed ERP averages over these subsamples. Then we directly tested the hit-miss difference topographies at the relevant time points (50 ms, 80 ms, 100 ms, 140 ms, and 300 ms), within each group using a Bayesian paired-sample *t*-test equivalent, and between the two groups using a Bayesian two-sample *t*-test equivalent (Krekelberg, 2022). Note that insofar as the hit-miss contrast constitutes a proxy measure of perceptual accuracy, it captures an important aspect of this phenomenon. For the P50, we found evidence (BF10 $\geq$ 3) for a hit-miss difference within the tactile group in the relevant electrodes, but no evidence (BF10 $<$ 3) in any electrode for a hit-miss difference within the electrical group, nor for a between-groups difference. However, the plots reveal considerable variability in P50 peak latencies both within and between the groups, which are likely to exaggerate the hit-miss difference especially in the electrical group, thereby reducing the between-groups difference. Therefore, we repeated the analysis for the hit-miss topographies at the actual peak times (tactile hit: 48.8 ms; tactile miss: 62.5 ms; electrical hit: 54.7 ms; electrical miss: 58.6 ms). Under these conditions, the hit-miss difference in the tactile group becomes stronger and more widespread, and there is evidence for a hit-miss difference in the electrical group in AF4 and ipsilateral electrode

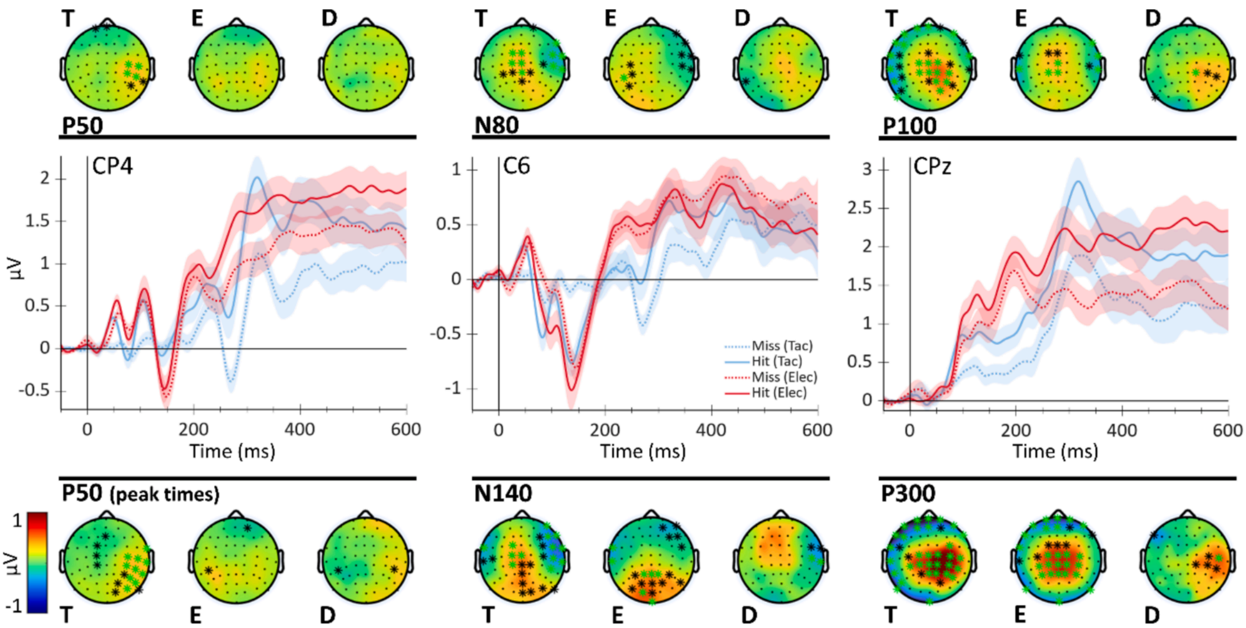

Fig. 7. Comparison of raw-voltage hit-miss difference maps within and between the tactile (blue) and electrical (red) groups. 40 intensity-matched (equal number of hit and miss trials within each of the 10 intensity levels) subsamples per participant (for a total of 1000 in each group of n = 25) were randomly drawn, and subject-level ERP averages across subsamples computed. The purpose of intensity-matching was to reduce the intensity confound inherent in our design, and the purpose of averaging multiple subsamples was to increase the reliability of the analysis by reducing sampling bias (note that both steps are unnecessary in our main analysis using Bayesian model selection). The middle panel shows grand-averaged ERP plots, which are highly similar to the single subsample plots shown in Fig. 4. Topographies show the results of two-tailed paired-sample Bayesian *t*-test equivalents for the hit-miss difference within the tactile (T) and electrical (E) groups, and of two-tailed two-sample Bayesian *t*-test equivalents for the between-groups difference (D) (Krekelberg, 2022). Black asterisks represent BF10 $\geq$ 3, green asterisks represent BF10 $\geq$ 10. Time points were chosen as 50 ms (P50), 80 ms (N80), 100 ms (P100), 140 ms (N140), and 300 ms (P300). For the P50, an additional test was carried out (lower left panel), using as time points the actual grand-average peak latencies (tactile hit: 48.8 ms; tactile miss: 62.5 ms; electrical hit: 54.7 ms; electrical miss: 58.6 ms).

CP5, but not in contralateral electrodes, while there is evidence for a between-groups difference in CP5 and contralateral CP6. The other components agree well with the BMS results, except for a between-groups difference for the N140 in contralateral frontocentral electrodes that is very likely caused by the much stronger hit-miss difference in the tactile group. However, raw voltage differences do not directly correspond to exceedance probabilities, and it is entirely possible that the same model performs best in both groups even though the raw voltage difference between hits and misses differs between the two groups. This is because subtler differences can be captured by a more sensitive single-trial modelling approach such as the one we used in our main analysis. Overall, the results of this control analysis directly support our conclusions and help to put our main results in perspective, even though several aspects of the analyses are not directly comparable.

4. Discussion

In this study, we used single-trial modelling and BMS within and between groups to investigate how mechanical and electrical stimulation, under otherwise largely identical conditions, differentially affect the event-related potentials associated with somatosensory target detection, while controlling for the influence of task-relevance and post-perceptual processes. We found strong differences in model performances between the two groups that were most pronounced in the time ranges of the P50, P100, and P300 components, while they were more similar in the N80 and N140 time ranges. The between-groups analysis confirmed that these findings were due to group differences.

4.1. P50

The P50 component in the electrical group was present for both hits and misses, and was best explained by stimulus intensity. In striking contrast, while there was a P50 for detected targets in the tactile group, this component was largely absent when targets were not detected, and this was reflected in the BMS results, where the binary detection model outperformed all other models in the P50 time range. This result is in line with the finding by Soininen and Järvilehto (1983), who had mechanically stimulated the hairy skin of the back of the hand and found P50, P100, N190, and P400 only for detected trials. It is also in line with almost all threshold detection studies using electrical stimulation (both of fingers and of the median nerve), which found no differences in the P50 time range for hits compared to misses (Auksztulewicz et al., 2012; Schubert et al., 2006; Uemura et al., 2021; Zhang & Ding, 2009), with some studies showing that P50 amplitudes vary with physical stimulus intensity instead (Forschack et al., 2020; Nierhaus et al., 2015; Schröder et al., 2021). The same linear scaling effect has been reported for early magnetic SI responses to electrical stimuli (Jousmäki & Forss, 1998; Torquati et al., 2002), including the P50m/P60m (Lin et al., 2003), which is seen as the direct magnetic analogue of the electrophysiological P50 (Wikström et al., 1996). Crucially however, our finding shows that the results achieved using electrical stimulation, beginning with Libet et al. (1967), may not hold generally, but may instead be peculiar to studies using this particular stimulation type.

The question to be addressed is why the P50 amplitude is predictive of detection for tactile, but not electrical stimulation. An obvious difference between the two stimulation types lies in how they affect the physiological pathways leading from the index finger to SI. The human fingertip contains four types of cutaneous low-threshold mechanoreceptors (LTMRs), innervated by four types of afferent Aβ fibers, all of which have different preferred stimulus types and activation thresholds (Handler & Ginty, 2021; Johnson, 2001). The brief mechanical impulse of the piezoelectrically driven pin during tactile stimulation is likely to preferentially activate the Meissner's corpuscles innervated by type 1 rapidly adapting fibers (RA1 units) and, possibly, Merkel cell-neurite complexes innervated by type 1 slowly adapting fibers (SA1 units) in the superficial skin of the fingertip which respond best to single impulses, but probably only to a much lesser degree the more deeply located Pacinian corpuscles and Ruffini endings (innervated by type 2 RA and SA fibers, respectively). RA2 units (Pacinians) have extremely low activation thresholds for stimuli in their optimal frequency range around 250 Hz, but for frequencies below 50 Hz (let alone single impulses), their thresholds are much higher than those of the RA1 and SA1 units, while SA2 units (Ruffinis) respond best to sustained skin stretch (Johansson & Vallbo, 1983; Johnson, 2001; Mountcastle et al., 1972). In contrast, the effects of electrical stimulation will impact non-specifically on all local fibers, bypassing receptors of all types (Mauguière, 2003; Poletto, 2006). An electrically induced swath of activity arriving at SI may therefore be more likely than a mechanically induced swath to generate measurable potentials already for subthreshold stimulation. Equally importantly, neural activation thresholds coincide with psychophysical detection thresholds only in some, not in all types of LTMR afferents. Microneurography studies (Vallbo & Hagbarth, 1968) have suggested such a correspondence between sensory and subjective detection thresholds for RA1 units in the glabrous skin (Johansson & Vallbo, 1979) and SA1 units in the hairy skin (Järvilehto et al., 1981). In these, but not in the other two receptor types, extremely sparse peripheral input can be sufficient to induce conscious detection. Studies combining microneurography with intraneural microstimulation (INMS) have found that a single impulse in a single RA1 unit (but not in any of the other types) in the glabrous skin can sometimes induce a conscious percept (Johansson & Vallbo, 1983; Torebjörk & Ochoa, 1980; Vallbo & Johansson, 1984). Based on these results, Soininen and Järvilehto (1983) already proposed that the tactile P50 response may be triggered by this peripheral activity volley and may be related to conscious perception.

These facts suggest the following hypothesis regarding the different dynamics of the tactile- and electrical-evoked P50: with electrical stimulation, the P50 scales with intensity already for subliminal stimulation, because some non-RA1 fibers with low activation thresholds are already being activated, leading to the observed subliminal cortical potentials (Forschack et al., 2020; Libet et al., 1967; Nierhaus et al., 2015; Ray et al., 1999; Schröder et al., 2021). Presumably, many of these fibers are of the extremely sensitive RA2 type. Under ecological stimulation conditions, the Pacini corpuscle endings, acting as high-pass filters (Mountcastle et al., 1990), would allow only high-frequency vibrotactile stimuli to activate these fibers, but electrical stimulation bypasses this filter (Poletto, 2006). With mechanical stimulation, on the other hand, these fibers remain largely silent, so that the P50 occurs only once the RA1 units are activated; and because in these units the neural activation and psychophysical thresholds coincide, the P50 correlates with subjective detection with this stimulation type. With electrical stimulation, this binary transition is essentially masked by subthreshold activations of other units. When the median nerve at the wrist instead of the fingertip is stimulated, this masking phenomenon may play out even stronger, because an even greater variety of nerve types (including sensory, proprioceptive, and afferent motor fibers) are targeted at this site (Koivikko, 1971). This is in line with the results of Schröder et al. (2021), where the intensity model generally scored higher EPs, and the P50 intensity effect had a much greater spatial extent than in our experiment. It may also help to explain why two studies found early activity to be predictive of detection despite using electrical stimulation (Hirvonen & Palva, 2016; Palva et al., 2005). Both these studies were conducted using MEG. Importantly, MEG is sensitive mainly to sources tangential to the scalp, that is, to activity coming predominantly from the cortical sulci, whereas EEG tracks activity from both gyri and sulci (Hämäläinen et al., 1993). EEG may thus be more susceptible to the described masking effect, because it picks up more of the additional subthreshold SI activity induced by electrical stimulation than MEG does.

What processes, then, does the P50 reflect, and how, if at all, is it related to somatosensory target detection? Most authors believe that potentials in the P50 latency range are too early to directly reflect endogenous processing of the stimulus, and, to the extent that they are predictive of perceptual outcomes, rather reflect the prestimulus attentional state, anticipation of, and/or expectations about the stimulus (Desmedt & Tomberg, 1989; Josiassen et al., 1982). The P50/P60m has been proposed in part to reflect inhibitory processing (Wikström et al., 1996) that sharpens the initial thalamo-cortical input (itself reflected by the N20) with respect to (in- or extrinsic) noise (Nierhaus et al., 2015; Pleger & Villringer, 2013). While inhibitory processing is initiated already for subthreshold stimuli, it would then have to reach a sufficient level in order to enable conscious perception. In the limit, this level appears to be achievable by a single RA1 action potential reaching SI. This proposal matches well with the reported scaling of the P50 with stimulus intensity (Forschack et al., 2020), and it can also accommodate the enhancement of the P50 by attention (Desmedt et al., 1983; Forschack et al., 2017; Josiassen et al., 1982, 1990), which in this light appears as an attentional modulation of inhibitory networks in SI.

Importantly, this does not necessarily mean that the P50 is an NCC proper, as opposed to a mere prerequisite of consciousness (Aru et al., 2012; de Graaf et al., 2012). Overall, it seems likely that more complex processing following the RA-mediated sharpening response in SI is necessary to render the stimulus conscious, as we discuss next.

4.2. The N80-N140 complex

For mechanical but not electrical stimulation, we found a prominent N80 component for hits compared to misses over C6 and proximal electrodes that was followed by a separate N140 in the same electrode region. In the electrical group, the N80 and N140 were less clearly separable and appeared to constitute a single negative deflection. A component similar to the N80 has often been described in studies using strong electrical (Allison et al., 1992; Desmedt et al., 1983; Goff et al., 1962; Michie et al., 1987) or mechanical stimulation (Eimer & Forster, 2003; Guidotti et al., 2023; Hämäläinen et al., 1990; Schubert et al., 2008; Taylor-Clarke et al., 2002; Zopf et al., 2004). In both groups in our study, the EEG signal in the N80 and N140 time ranges was best explained by similar frontocentral to frontal effect clusters with the detection model performing best in the anterior, and the detection probability model performing best in the posterior electrodes of these clusters, although the detection effect in the electrical group was spatially more restricted. As noted above, the sigmoidal detection probability model occupies a middle ground between the intensity and detection models. Since the scalp-recorded signal is the sum of the activity of entire neuronal populations, the detection probability model might reflect the activity of mixed neuronal populations that contain different types of neurons, some with sensory and some with categorical response characteristics, as well as combinations thereof. Notably, such a population type has been observed in monkey SII, and has been hypothesized to play a role in the transition from sensory to perceptual processing (Rossi-Pool et al., 2021). While the N80 was not unambiguously separable from the N140 in the electrical group in our data, it is noteworthy that the electrical N140 deflection began already around 60 ms, at the same time as the tactile N80, and was slightly bimodal, i.e., had a small peak already before the main peak at ~140 ms. Interestingly, an occasionally bimodal N140 has been reported already by Goff et al. (1962), who compared somatosensory-evoked potentials to supra-threshold stimulation of the median nerve at the wrist and the index finger, as well as by Hämäläinen et al. (1990), who used mechanical stimulation of the middle finger. It is also discernible in somatosensory masking (Schubert et al., 2006) and *peri*-threshold detection studies (Forschack et al., 2020; Schröder et al., 2021), but has frequently gone unnoticed. In some of these studies, the first of the two peaks is strongly reminiscent of the effect at 80 ms reported by Auksztulewicz and colleagues (2012; 2013). It is well known that the peak latency of the N140 is rather variable, and it has also been shown that it is a complex component containing several subcomponents (Allison et al., 1992; García-Larrea et al., 1995; Zopf et al., 2004), potentially reflecting different processes. It is therefore possible that the N140 generally contains an earlier N80-like part that is difficult to separate from the N140 proper when electrical stimulation is used, but becomes more obvious with mechanical stimulation. Allison et al. (1992) observed that the electrically-induced N70 is only recordable in isolation at rather short ISIs, and "appears to be obscured by other long-latency activity" (p. 311) for longer ISIs, typically used in NCC studies (including the present one). The MEG study by Jones et al. (2007), who used tactile threshold stimulation and investigated the response time course of a dipole localized to contralateral SI using a biophysical model, found that the earliest deflection predictive of subjective detection was a negative M70 component which transitioned into a positive-going M135 deflection. Both responses were likely driven by excitatory feedback input from SII, with the M135 requiring additional thalamic input, which in turn was presumably driven by cortico-thalamic feedback, again likely involving SII. Based on these modelling results, Jones et al. (2007) suggest that the M70 probably corresponds to the intra-cortically recorded N1 component found in monkeys for hits compared to misses in a detection task for both mechanical and electrical stimulation (Cauller & Kulics, 1991). There, the difference between the two stimulation types was that electrical stimulation activated a much larger horizontal (intra-layer) area of SI than mechanical stimulation, whereas the mechanically evoked N1 was more focal but also had a larger peak amplitude. These characteristics seem to match well with those of the scalp-level signals recorded in our study, where the tactile N80 peak is very prominent, while the corresponding first N140 peak during electrical stimulation is less discernible, and appears as part of the N140 component. Our tactile N80 may therefore correspond to the M70 of Jones et al. (2007) and the N1 of Cauller and Kulics (1991), while the M135, into which the M70 transitions, may correspond to the N140 proper. Given that the detection-predictive M70/N1/N80 seems to be heavily driven by cortico-cortical and cortico-thalamo-cortical feedback loops involving sensory cortices, and Auksztulewicz and colleagues (2012; 2013) have provided evidence for a complex origin of the N140 involving recurrent processing between SI and SII, the N80/N140 complex would be a natural candidate for an NCC according to recurrent processing theory (Lamme, 2020; Lamme & Roelfsema, 2000), which posits precisely this feature as a hallmark of consciousness. Interestingly, one recent study recorded single-neuron activity from the human thalamus and subthalamic nucleus, and found neurons whose firing rate correlated with conscious detection of vibrotactile stimuli 150 ms and 300 ms after stimulus onset, directly suggesting cortico-thalamo-cortical loops in the N140 and P300 time ranges (Pereira et al., 2025). The mechanistic role of such loops has been suggested to consist in the coupling of apical dendritic and somatic compartments of layer 5 pyramidal cells in sensory cortices, mediated by matrix cells of the non-specific thalamus (Aru et al., 2020; Bachmann et al., 2020; Phillips et al., 2025; Whyte et al., 2024), and a recent study confirmed that a computational model simulating this mechanism can reproduce the behavioral and neural signatures of conscious somatosensory threshold detection in a mouse model (Whyte et al., 2025). A decisive role of SII in conscious somatosensory detection is also suggested by several recent human intracortical stereo-EEG (Albertini et al., 2025; Del Vecchio et al., 2019, Del Vecchio et al., 2021) and functional magnetic resonance imaging (fMRI) studies (Grund et al., 2021; Moore et al., 2013; Peters et al., 2023; Schröder et al., 2019); however, these results were achieved using electrical median nerve or finger stimulation, and our results show that they may not be straightforwardly generalizable to mechanical stimulation. In sum, however, both empirical and theoretical developments speak against the sufficiency of early SI activity, and for a complex interplay of SI, SII, and the thalamus as the mechanism underlying conscious somatosensory perception.

4.3. P100 and P300

The P100 was best explained by detection in the tactile group, and by detection probability in the electrical group in our study. When considering only electrode CPz, the latter result appears to diverge from the one achieved by Schröder et al. (2021) using median nerve stimulation. However, the global profile of the P100 effect is similar between the two studies, with a central cluster whose ipsilateral side is dominated by detection probability, and the contralateral side by stimulus intensity. The main difference is that intensity effects are overall much stronger with median nerve stimulation, while the intensity effect is restricted to electrode C2 with fingertip stimulation, which exhibits BMS results (see online supplement, Fig. S1) virtually identical to electrode CPz in Schröder et al. (2021). The presence of a detection effect in the tactile group and its absence in the electrical group are in line with the threshold detection study by Jones et al. (2007) using mechanical stimuli and with several other threshold detection studies that used electrical stimulation and reported little or no trace of such an effect on the P100 (Auksztulewicz et al., 2012; Auksztulewicz & Blankenburg, 2013; Schröder et al., 2021). The one study that found a clear detection effect on the P100 in response to electrical fingertip stimulation used a masking paradigm, which may explain the divergent finding (Schubert et al., 2006).

The P300 has been considered a hallmark of conscious processing in the framework of Global Neuronal Workspace theory (Dehaene & Naccache, 2001; Mashour et al., 2020) until more recent studies showed that it reflects post-perceptual processes more closely (Dellert et al., 2021; Pitts et al., 2014; Schlossmacher et al., 2021; Schröder et al., 2021). In threshold detection tasks, it reflects somatosensory awareness both categorically (Auksztulewicz et al., 2012) and parametrically (Auksztulewicz & Blankenburg, 2013) but ceases to do so when post-perceptual processes are controlled with a matching task (Schröder et al., 2021). The results from our electrical group largely concur with this latter finding with regard both to the plateau-like P300 morphology and the BMS results, with the difference that the detection model explains the final data segments of the epoch, beginning at ~550 ms. However, the latency of this detection effect is certainly too long to challenge the main conclusion reached by Schröder et al. (2021), i.e., that the P300 is not a reliable marker of somatosensory target detection. Surprisingly however, the results from our tactile group, where the detection model outperformed all other models across the P300 time range, seem to restrict that conclusion to experiments using electrical stimulation, be it of the median nerve or the fingertip. Since the matching task was employed in both groups and, hence, task-relevance was controlled equally in both groups, the observed difference is most likely attributable to the different stimulation conditions. Nakajima & Imamura (2000) have shown that the somatosensory-evoked P300 has (at least) an endogenous and an exogenous component, in that its amplitude is modulated by attention, but also stimulus intensity. A scaling of the P300 amplitude with intensity is observable in our data as well in both groups. Our BMS results however suggest that, for tactile stimuli, the balance between exo- and endogenous influences on the P300 may be shifted toward the latter. This may occur for the same reasons as discussed above regarding the P50. Alouit et al. (2025) found different functional connectivity patterns between electrical and tactile stimulation across the P50 and P100 time ranges, pointing to different modes of cortical processing. Although they did not investigate later time ranges, it is easily conceivable that these different modes persist, and influence later processes in the P300 time range. An additional, rather speculative, explanation might be that comparatively "naturalistic" tactile stimuli are of greater potential relevance and, consequently, salience than "artificial" electrical stimuli for the somatosensory system, so that a categorical perceptual representation gains in importance when the former are processed. However, it can just as well be argued that the unusual electrical stimulation should be more salient, and at any rate the task-relevance should be the same in both groups in our study. Nevertheless, it might be interesting further to pursue the path toward greater ecological validity in future studies of somatosensory awareness.

4.4. Limitations and future directions

Some limitations of our study should be considered. First, because our design permits no distinction between correct and incorrect responses, the influence of objective task performance (Lamy et al., 2008) could not be analyzed, nor were we able to separate participants' response criterion from their sensitivity (Green & Swets, 1966), precluding criterion-based inferences about the influence of decision confidence (Salti et al., 2012). We tried to ensure high task performance by inviting only well-trained participants, and found no influence of subjective uncertainty (confidence) as modeled with an inverted u-shaped regressor, but future studies with suitable designs should address these aspects more directly. Second, all our analyses were done in the time domain, and we consequently had no way of detecting non-phase-locked, oscillatory effects. Many studies have found relationships between somatosensory target detection and pre-stimulus power or phase in the alpha and beta frequency ranges (Ai & Ro, 2013; Craddock et al., 2017; Forschack et al., 2020; Linkenkaer-Hansen et al., 2004; Weisz et al., 2014), different functional interpretations have been given to the different frequency bands (Engel & Fries, 2010), and their mutual interactions are increasingly being explored (Fries, 2015; Siegel et al., 2012). Our study was not designed for time–frequency analyses, and our short ITI of (at minimum) 0.7 s complicates uncontaminated analysis of the pre-stimulus period, particularly for the lower frequencies. However, it would be of great interest for future studies to investigate the differences between threshold detection with tactile and electrical stimulation in the time–frequency domain, potentially also finding relationships between pre-stimulus oscillatory activity and ERP components (Nikouline et al., 2000; Trajkovic et al., 2024; Zhang & Ding, 2009). It is also noteworthy that ITIs are periods of active neuro-cognitive processing rather than neutral breaks (e.g., Compton et al., 2011), and it has been shown that short ITIs (around 700 ms) can negatively impact error monitoring and reduce differences of error-related neural measures between correctly and incorrectly answered trials in a Stroop task, in both the time and frequency domains (Compton et al., 2017). While participants had no possibility of monitoring perceptual errors in our design, it is conceivable that ITI durations also interact with perceptual thresholds and/or neural processing during the ITI. This possibility warrants further investigation in future studies. Finally, like Alouit et al. (2025), our study used a between-subjects design, leaving open the possibility of differences between the tactile and electrical participant samples being partly responsible for the effects we found. While we regard it as rather unlikely that such differences should be systematic between two very homogeneous samples from the pool of university students, we cannot ultimately rule out this possibility, and future studies should also employ within-subject designs.

5. Conclusion

In conclusion, our study indicates that the correlates of somatosensory threshold detection strongly depend on the type of stimulation used. Most importantly, the P50 component, which has until now been considered to reflect physical stimulus attributes, is predictive of conscious detection under physiological conditions, i.e., when using more ecologically valid tactile as opposed to "artificial" electrical stimulation, and therefore most likely reflects a prerequisite of conscious perception that cannot be ascertained under electrical stimulation. Moreover, our results tend to corroborate the N140 as a robust NCC with both types of stimulation, with a pronounced N80-N140 partition in the tactile case that is less evident in the electrical case. Finally, the differential modulation of the P100 and P300 between the two groups in our data suggests that the degree to which this component reflects perceptual or post-perceptual processes, respectively, may likewise depend on the type of stimulation, once again illustrating the susceptibility of putative somatosensory NCCs to different stimulation protocols.

CRediT authorship contribution statement

Jona Förster: Writing – review & editing, Writing – original draft, Visualization, Software, Methodology, Investigation, Formal analysis, Conceptualization. **Giovanni Vardiero:** Writing – review & editing, Investigation. **Till Nierhaus:** Writing – review & editing, Supervision, Conceptualization. **Felix Blankenburg:** Writing – review & editing, Supervision, Methodology, Conceptualization.

Declaration of competing interest

The authors declare that they have no known competing financial interests or personal relationships that could have appeared to influence the work reported in this paper.

Appendix A. Supplementary data

Supplementary data to this article can be found online at https://doi.org/10.1016/j.concog.2025.103935.

Data availability

Data will be made available on request.

References

Ai, L., & Ro, T. (2013). The phase of prestimulus alpha oscillations affects tactile perception. *Journal of Neurophysiology, 111*(6), 1300–1307. https://doi.org/10.1152/jn.00125.2013

Albert, J. H. (1997). Bayesian Testing and Estimation of Association in a Two-Way Contingency Table. *Journal of the American Statistical Association, 92*(438), 685–693. https://doi.org/10.2307/2965716

Albertini, D., Vecchio, M. D., Sartori, I., Pigorini, A., Talami, F., Zauli, F. M., Sarasso, S., Mikulan, E. P., Massimini, M., & Avanzini, P. (2025). Conscious tactile perception entails distinct neural dynamics within somatosensory areas. *Current Biology*. https://doi.org/10.1016/j.cub.2025.04.052

Allison, T., McCarthy, G., & Wood, C. C. (1992). The relationship between human long-latency somatosensory evoked potentials recorded from the cortical surface and from the scalp. *Electroencephalography and Clinical Neurophysiology/Evoked Potentials Section, 84*(4), 301–314. https://doi.org/10.1016/0168-5597(92)90082-M

Alouit, A., Gavaret, M., Ramdani, C., Lindberg, P. G., & Dupin, L. (2025). Cortical activations induced by electrical versus vibrotactile finger stimulation using EEG. *NeuroImage, 314*, Article 121249. https://doi.org/10.1016/j.neuroimage.2025.121249

Aru, J., Bachmann, T., Singer, W., & Melloni, L. (2012). Distilling the neural correlates of consciousness. *Neuroscience & Biobehavioral Reviews, 36*, 737–746. https://doi.org/10.1016/j.neubiorev.2011.12.003

Aru, J., Suzuki, M., & Larkum, M. E. (2020). Cellular Mechanisms of Conscious Processing. *Trends in Cognitive Sciences, 24*(10), 814–825. https://doi.org/10.1016/j.tics.2020.07.006

Auksztulewicz, R., & Blankenburg, F. (2013). Subjective rating of weak tactile stimuli is parametrically encoded in event-related potentials. *Journal of Neuroscience, 33*(29), 11878–11887. https://doi.org/10.1523/JNEUROSCI.4243-12.2013

Auksztulewicz, R., Spitzer, B., & Blankenburg, F. (2012). Recurrent neural processing and somatosensory awareness. *Journal of Neuroscience, 32*(3), 799–805. https://doi.org/10.1523/JNEUROSCI.3974-11.2012

Bachmann, T., Suzuki, M., & Aru, J. (2020). Dendritic integration theory: A thalamo-cortical theory of state and content of consciousness. Article II *Philosophy and the Mind Sciences, 1*(II). https://doi.org/10.33735/phimisci.2020.II.52.

Brainard, D. H. (1997). The psychophysics toolbox. *Spatial Vision, 10*(4), 433–436.

Cauller, L. J., & Kulics, A. T. (1991). The neural basis of the behaviorally relevant N1 component of the somatosensory-evoked potential in SI cortex of awake monkeys: Evidence that backward cortical projections signal conscious touch sensation. *Experimental Brain Research, 84*(3), 607–619. https://doi.org/10.1007/BF00230973

Compton, R. J., Arnstein, D., Freedman, G., Dainer-Best, J., & Liss, A. (2011). Cognitive control in the intertrial interval: Evidence from EEG alpha power. *Psychophysiology, 48*(5), 583–590. https://doi.org/10.1111/j.1469-8986.2010.01124.x

Compton, R. J., Heaton, E., & Ozer, E. (2017). Intertrial interval duration affects error monitoring. *Psychophysiology, 54*(8), 1151–1162. https://doi.org/10.1111/psyp.12877

Craddock, M., Poliakoff, E., El-deredy, W., Klepousniotou, E., & Lloyd, D. M. (2017). Pre-stimulus alpha oscillations over somatosensory cortex predict tactile misperceptions. *Neuropsychologia, 96*, 9–18. https://doi.org/10.1016/j.neuropsychologia.2016.12.030

Crick, F., & Koch, C. (1990). Towards a neurobiological theory of consciousness. *Seminars in the Neurosciences, 2*, 263–275.

Daunizeau, J., Adam, V., & Rigoux, L. (2014). VBA: A probabilistic treatment of nonlinear models for neurobiological and behavioural data. *PLOS Computational Biology, 10*(1), Article e1003441. https://doi.org/10.1371/journal.pcbi.1003441

de Graaf, T. A., Hsieh, P. J., & Sack, A. T. (2012). The 'correlates' in neural correlates of consciousness. *Neuroscience & Biobehavioral Reviews, 36*, 191–197. https://doi.org/10.1016/j.neubiorev.2011.05.012

Dehaene, S., & Naccache, L. (2001). Towards a cognitive neuroscience of consciousness: Basic evidence and a workspace framework. *Cognition, 79*(1), 1–37. https://doi.org/10.1016/S0010-0277(00)00123-2

Del Vecchio, M., Caruana, F., Sartori, I., Pelliccia, V., Lo Russo, G., Rizzolatti, G., & Avanzini, P. (2019). Ipsilateral somatosensory responses in humans: The tonic activity of SII and posterior insular cortex. *Brain Structure and Function, 224*(1), 9–18. https://doi.org/10.1007/s00429-018-1754-6

Del Vecchio, M., Fossataro, C., Zauli, F. M., Sartori, I., Pigorini, A., d'Orio, P., Abarrategui, B., Russo, S., Mikulan, E. P., Caruana, F., Rizzolatti, G., Garbarini, F., & Avanzini, P. (2021). Tonic somatosensory responses and deficits of tactile awareness converge in the parietal operculum. *Brain, 144*(12), 3779–3787. https://doi.org/10.1093/brain/awab384

Dellert, T., Müller-Bardorff, M., Schlossmacher, I., Pitts, M., Hofmann, D., Bruchmann, M., & Straube, T. (2021). Dissociating the neural correlates of consciousness and task relevance in face perception using simultaneous EEG-fMRI. *Journal of Neuroscience, 41*(37), 7864–7875. https://doi.org/10.1523/JNEUROSCI.2799-20.2021

Desmedt, J. E., Huy, N. T., & Bourguet, M. (1983). The cognitive P40, N60 and P100 components of somatosensory evoked potentials and the earliest electrical signs of sensory processing in man. *Electroencephalography and Clinical Neurophysiology, 56*(4), 272–282. https://doi.org/10.1016/0013-4694(83)90252-3

Desmedt, J. E., & Tomberg, C. (1989). Mapping early somatosensory evoked potentials in selective attention: Critical evaluation of control conditions used for titrating by difference the cognitive P30, P40, P100 and N140. *Electroencephalography and Clinical Neurophysiology, 74*(5), 321–346. https://doi.org/10.1016/0168-5597(89)90001-4

Eimer, M., & Forster, B. (2003). Modulations of early somatosensory ERP components by transient and sustained spatial attention. *Experimental Brain Research, 151*(1), 24–31. https://doi.org/10.1007/s00221-003-1437-1

Engel, A. K., & Fries, P. (2010). Beta-band oscillations—signalling the status quo? *Current Opinion in Neurobiology, 20*(2), 156–165. https://doi.org/10.1016/j.conb.2010.02.015

Forschack, N., Nierhaus, T., Müller, M. M., & Villringer, A. (2017). Alpha-band brain oscillations shape the processing of perceptible as well as imperceptible somatosensory stimuli during selective attention. *Journal of Neuroscience, 37*(29), 6983–6994. https://doi.org/10.1523/JNEUROSCI.2582-16.2017

Forschack, N., Nierhaus, T., Müller, M. M., & Villringer, A. (2020). *Dissociable neural correlates of stimulation intensity and detection in somatosensation., NeuroImage, 217*, Article 116908. https://doi.org/10.1016/j.neuroimage.2020.116908

Forss, N., Hari, R., Salmelin, R., Ahonen, A., Hämäläinen, M., Kajola, M., Knuutila, J., & Simola, J. (1994). Activation of the human posterior parietal cortex by median nerve stimulation. *Experimental Brain Research, 99*(2), 309–315. https://doi.org/10.1007/BF00239597

Forss, N., Salmelin, R., & Hari, R. (1994). Comparison of somatosensory evoked fields to airpuff and electric stimuli. *Electroencephalography and Clinical Neurophysiology/Evoked Potentials Section, 92*(6), 510–517. https://doi.org/10.1016/0168-5597(94)90135-X

Förster, J., Koivisto, M., & Revonsuo, A. (2020). ERP and MEG correlates of visual consciousness: The second decade. *Consciousness and Cognition, 80*, Article 102917. https://doi.org/10.1016/j.concog.2020.102917

Förster, J., Nierhaus, T., Schröder, P., & Blankenburg, F. (2025). Perceptual experience in somatosensory temporal discrimination is indexed by a mid-latency fronto-central ERP difference. *Scientific Reports, 15*(1), 7674. https://doi.org/10.1038/s41598-025-91580-1

Fries, P. (2015). Rhythms for cognition: Communication through coherence. *Neuron, 88*(1), 220–235. https://doi.org/10.1016/j.neuron.2015.09.034

Friston, K. J., & Penny, W. (2003). Posterior probability maps and SPMs. *NeuroImage, 19*(3), 1240–1249. https://doi.org/10.1016/S1053-8119(03)00144-7

Frot, M., & Mauguière, F. (2003). Dual representation of pain in the operculo-insular cortex in humans. *Brain, 126*(2), 438–450. https://doi.org/10.1093/brain/awg032

García-Larrea, L., Lukaszewicz, A.-C., & Mauguière, F. (1995). Somatosensory responses during selective spatial attention: The N120-to-N140 trasition. *Psychophysiology, 32*(6), 526–537. https://doi.org/10.1111/j.1469-8986.1995.tb01229.x

Goff, W. R., Rosner, B. S., & Allison, T. (1962). Distribution of cerebral somatosensory evoked responses in normal man. *Electroencephalography and Clinical Neurophysiology, 14*(5), 697–713. https://doi.org/10.1016/0013-4694(62)90084-6

Green, D. M., & Swets, J. A. (1966). *Signal detection theory and psychophysics*. Wiley.

Grund, M., Forschack, N., Nierhaus, T., & Villringer, A. (2021). Neural correlates of conscious tactile perception: An analysis of BOLD activation patterns and graph metrics. *NeuroImage, 224*, Article 117384. https://doi.org/10.1016/j.neuroimage.2020.117384

Guidotti, M., Beaurieux, C., Marionnaud, P., Bonnet-Brilhault, F., Wardak, C., & Latinus, M. (2023). Skin type and nerve effects on cortical tactile processing: A somatosensory evoked potentials study. *Journal of Neurophysiology, 130*(3), 547–556. https://doi.org/10.1152/jn.00444.2022

Hämäläinen, H., Kekoni, J., Sams, M., Reinikainen, K., & Näätänen, R. (1990). Human somatosensory evoked potentials to mechanical pulses and vibration: Contributions of SI and SII somatosensory cortices to P50 and P100 components. *Electroencephalography and Clinical Neurophysiology, 75*(1), 13–21. https://doi.org/10.1016/0013-4694(90)90148-D

Hämäläinen, M., Hari, R., Ilmoniemi, R. J., Knuutila, J., & Lounasmaa, O. V. (1993). Magnetoencephalography—Theory, instrumentation, and applications to noninvasive studies of the working human brain. *Reviews of Modern Physics, 65*(2), 413–497. https://doi.org/10.1103/RevModPhys.65.413

Handler, A., & Ginty, D. D. (2021). The mechanosensory neurons of touch and their mechanisms of activation. *Nature Reviews Neuroscience, 22*(9), 521–537. https://doi.org/10.1038/s41583-021-00489-x

Hensel, H., & Boman, K. K. A. (1960). Afferent impulses in cutaneous sensory nerves in human subjects. *Journal of Neurophysiology, 23*, 564–578.

Hirvonen, J., & Palva, S. (2016). Cortical localization of phase and amplitude dynamics predicting access to somatosensory awareness. *Human Brain Mapping, 37*(1), 311–326. https://doi.org/10.1002/hbm.23033

Houweling, A. R., & Brecht, M. (2008). Behavioural report of single neuron stimulation in somatosensory cortex. *Nature, 451*(7174), 65–68. https://doi.org/10.1038/nature06447

Ille, N., Berg, P., & Scherg, M. (2002). Artifact correction of the ongoing EEG using spatial filters based on artifact and brain signal topographies. *Journal of Clinical Neurophysiology, 19*(2), 113–124.

Järvilehto, T., Hämäläinen, H., & Soininen, K. (1981). Peripheral neural basis of tactile sensations in man: II. Characteristics of human mechanoreceptors in the hairy skin and correlations of their activity with tactile sensations. *Brain Research, 219*(1), 13–27. https://doi.org/10.1016/0006-8993(81)90264-X

Johansson, R. S., & Vallbo, Å. B. (1979). Detection of tactile stimuli. Thresholds of afferent units related to psychophysical thresholds in the human hand. *The Journal of Physiology, 297*(1), 405–422. https://doi.org/10.1113/jphysiol.1979.sp013048

Johansson, R. S., & Vallbo, Å. B. (1983). Tactile sensory coding in the glabrous skin of the human hand. *Trends in Neurosciences, 6*, 27–32. https://doi.org/10.1016/0166-2236(83)90011-5

Johnson, K. O. (2001). The roles and functions of cutaneous mechanoreceptors. *Current Opinion in Neurobiology, 11*(4), 455–461. https://doi.org/10.1016/S0959-4388(00)00234-8

Jones, S. R., Pritchett, D. L., Stufflebeam, S. M., Hämäläinen, M., & Moore, C. I. (2007). Neural correlates of tactile detection: A combined magnetoencephalography and biophysically based computational modeling study. *Journal of Neuroscience, 27*(40), 10751–10764. https://doi.org/10.1523/JNEUROSCI.0482-07.2007

Josiassen, R. C., Shagass, C., Roemer, R. A., Ercegovac, D. V., & Straumanis, J. J. (1982). Somatosensory Evoked potential changes with a Selective attention Task. *Psychophysiology, 19*(2), 146–159. https://doi.org/10.1111/j.1469-8986.1982.tb02536.x

Josiassen, R. C., Shagass, C., Roemer, R. A., Slepner, S., & Czartorysky, B. (1990). Early cognitive components of somatosensory event-related potentials. *International Journal of Psychophysiology, 9*(2), 139–149. https://doi.org/10.1016/0167-8760(90)90068-O

Jousmäki, V., & Forss, N. (1998). Effects of stimulus intensity on signals from human somatosensory cortices. *Neuroreport, 9*(15), 3427.

Kass, R. E., & Raftery, A. E. (1995). Bayes Factors. *Journal of the American Statistical Association, 90*(430), 773–795. https://doi.org/10.1080/01621459.1995.10476572

Koivikko, M. J. (1971). Differences in evoked potentials to median and radial nerve stimulation in man. *Brain Research, 30*(1), 223–227. https://doi.org/10.1016/0006-8993(71)90021-7

Krekelberg, B. (2022). *BayesFactor (Version Release v2.3.0, available at.* [Computer software].

Kulics, A. T. (1982). Cortical neural evoked correlates of somatosensory stimulus detection in the rhesus monkey. *Electroencephalography and Clinical Neurophysiology, 53*(1), 78–93. https://doi.org/10.1016/0013-4694(82)90108-0

Lamme, V. A. F. (2020). Visual Functions Generating Conscious Seeing. *Frontiers in Psychology, 11*. https://doi.org/10.3389/fpsyg.2020.00083.

Lamme, V. A. F., & Roelfsema, P. R. (2000). The distinct modes of vision offered by feedforward and recurrent processing. *Trends in Neurosciences, 23*(11), 571–579. https://doi.org/10.1016/S0166-2236(00)01657-X

Lamy, D., Salti, M., & Bar-Haim, Y. (2008). Neural correlates of subjective awareness and unconscious processing: An ERP study. *Journal of Cognitive Neuroscience, 21*(7), 1435–1446. https://doi.org/10.1162/jocn.2009.21064

Libet, B. (1993). *Neurophysiology of consciousness.* Springer Science & Business Media.

Libet, B., Alberts, W. W., Wright, E. W., & Feinstein, B. (1967). Responses of human somatosensory cortex to stimuli below threshold for conscious sensation. *Science, 158*(3808), 1597–1600. https://doi.org/10.1126/science.158.3808.1597

Lin, Y.-Y., Shih, Y.-H., Chen, J.-T., Hsieh, J.-C., Yeh, T.-C., Liao, K.-K., Kao, C.-D., Lin, K.-P., Wu, Z.-A., & Ho, L.-T. (2003). Differential effects of stimulus intensity on peripheral and neuromagnetic cortical responses to median nerve stimulation. *NeuroImage, 20*(2), 909–917. https://doi.org/10.1016/S1053-8119(03)00387-2

Linkenkaer-Hansen, K., Nikulin, V. V., Palva, S., Ilmoniemi, R. J., & Palva, J. M. (2004). Prestimulus oscillations enhance psychophysical performance in humans. *Journal of Neuroscience, 24*(45), 10186–10190. https://doi.org/10.1523/JNEUROSCI.2584-04.2004

Marchini, J., & Presanis, A. (2004). Comparing methods of analyzing fMRI statistical parametric maps. *NeuroImage, 22*(3), 1203–1213. https://doi.org/10.1016/j.neuroimage.2004.03.030

Mashour, G. A., Roelfsema, P., Changeux, J.-P., & Dehaene, S. (2020). Conscious processing and the global neuronal workspace hypothesis. *Neuron, 105*(5), 776–798. https://doi.org/10.1016/j.neuron.2020.01.026

Mauguière, F. (2003). Chapter 5 Somatosensory evoked responses. In M. Hallett (Ed.), *Handbook of Clinical Neurophysiology* (Vol. 1, pp. 45–75). Elsevier. https://doi.org/10.1016/S1567-4231(09)70153-4.

Mauguière, F., Merlet, I., Forss, N., Vanni, S., Jousmäki, V., Adeleine, P., & Hari, R. (1997). Activation of a distributed somatosensory cortical network in the human brain. a dipole modelling study of magnetic fields evoked by median nerve stimulation. Part I: Location and activation timing of SEF sources. *Electroencephalography and Clinical Neurophysiology/Evoked Potentials Section, 104*(4), 281–289. https://doi.org/10.1016/S0013-4694(97)00006-0

Michie, P. T., Bearparic, H. M., Crawford, J. M., & Glue, L. C. T. (1987). The effects of spatial selective attention on the somatosensory event-related potential. *Psychophysiology, 24*(4), 449–463. https://doi.org/10.1111/j.1469-8986.1987.tb00316.x

Moore, C. I., Crosier, E., Greve, D. N., Savoy, R., Merzenich, M. M., & Dale, A. M. (2013). Neocortical correlates of vibrotactile detection in humans. *Journal of Cognitive Neuroscience, 25*(1), 49–61. https://doi.org/10.1162/jocn_a_00315

Mountcastle, V. B., LaMotte, R. H., & Carli, G. (1972). Detection thresholds for stimuli in humans and monkeys: Comparison with threshold events in mechanoreceptive afferent nerve fibers innervating the monkey hand. *Journal of Neurophysiology, 35*(1), 122–136. https://doi.org/10.1152/jn.1972.35.1.122

Mountcastle, V. B., Steinmetz, M. A., & Romo, R. (1990). Frequency discrimination in the sense of flutter: Psychophysical measurements correlated with postcentral events in behaving monkeys. *Journal of Neuroscience, 10*(9), 3032–3044. https://doi.org/10.1523/JNEUROSCI.10-09-03032.1990

Mudrik, L., Hirschhorn, R., & Korisky, U. (2024). Taking consciousness for real: Increasing the ecological validity of the study of conscious vs. unconscious processes. *Neuron, 112*(10), 1642–1656. https://doi.org/10.1016/j.neuron.2024.03.031

Nakajima, Y., & Imamura, N. (2000). Relationships between attention effects and intensity effects on the cognitive N140 and P300 components of somatosensory ERPs. *Clinical Neurophysiology, 111*(10), 1711–1718. https://doi.org/10.1016/S1388-2457(00)00383-7

Nierhaus, T., Forschack, N., Piper, S. K., Holtze, S., Krause, T., Taskin, B., Long, X., Stelzer, J., Margulies, D. S., Steinbrink, J., & Villringer, A. (2015). Imperceptible somatosensory stimulation alters sensorimotor background rhythm and connectivity. *Journal of Neuroscience, 35*(15), 5917–5925. https://doi.org/10.1523/JNEUROSCI.3806-14.2015

Nikouline, V. V., Wikström, H., Linkenkaer-Hansen, K., Kesäniemi, M., Ilmoniemi, R. J., & Huttunen, J. (2000). Somatosensory evoked magnetic fields: Relation to pre-stimulus mu rhythm. *Clinical Neurophysiology, 111*(7), 1227–1233. https://doi.org/10.1016/S1388-2457(00)00291-1

Oldfield, R. C. (1971). The assessment and analysis of handedness: The Edinburgh inventory. *Neuropsychologia, 9*(1), 97–113. https://doi.org/10.1016/0028-3932(71)90067-4

Palva, S., Linkenkaer-Hansen, K., Näätänen, R., & Palva, J. M. (2005). Early neural correlates of conscious somatosensory perception. *Journal of Neuroscience, 25*(21), 5248–5258. https://doi.org/10.1523/JNEUROSCI.0141-05.2005

Penny, W., Stephan, K. E., Daunizeau, J., Rosa, M. J., Friston, K. J., Schofield, T. M., & Leff, A. P. (2010). Comparing families of dynamic causal models. *PLOS Computational Biology, 6*(3), Article e1000709. https://doi.org/10.1371/journal.pcbi.1000709

Pereira, M., Faivre, N., Bernasconi, F., Brandmeir, N., Suffridge, J. E., Tran, K., Wang, S., Finomore, V., Konrad, P., Rezai, A., & Blanke, O. (2025). *Subcortical correlates of consciousness with human single neuron recordings., eLife, 13*, Article RP95272. https://doi.org/10.7554/eLife.95272

Peters, A., Bruchmann, M., Dellert, T., Moeck, R., Schlossmacher, I., & Straube, T. (2023). Stimulus awareness is associated with secondary somatosensory cortex activation in an inattentional numbness paradigm. Article 1 *Scientific Reports, 13*(1). https://doi.org/10.1038/s41598-023-49857-w.

Phillips, W. A., Bachmann, T., Spratling, M. W., Muckli, L., Petro, L. S., & Zolnik, T. (2025). Cellular psychology: Relating cognition to context-sensitive pyramidal cells. *Trends in Cognitive Sciences, 29*(1), 28–40. https://doi.org/10.1016/j.tics.2024.09.002

Pitts, M. A., Padwal, J., Fennelly, D., Martínez, A., & Hillyard, S. A. (2014). Gamma band activity and the P3 reflect post-perceptual processes, not visual awareness. *NeuroImage, 101*, 337–350. https://doi.org/10.1016/j.neuroimage.2014.07.024

Pleger, B., & Villringer, A. (2013). The human somatosensory system: From perception to decision making. *Progress in Neurobiology, 103*, 76–97. https://doi.org/10.1016/j.pneurobio.2012.10.002

Poletto, C. J. (2006). Tactile Stimulation. In *Encyclopedia of Medical Devices and Instrumentation*. John Wiley & Sons, Ltd. https://doi.org/10.1002/0471732877.emd319.

Pratt, H., Starr, A., Amlie, R. N., & Politoske, D. (1979). Mechanically and electrically evoked somatosensory potentials in normal humans. *Neurology, 29*(9 Pt 1), 1236–1244. https://doi.org/10.1212/wnl.29.9_part_1.1236

Ray, P. G., Meador, K. J., Smith, J. R., Wheless, J. W., Sittenfeld, M., & Clifton, G. L. (1999). Physiology of perception: Cortical stimulation and recording in humans. *Neurology, 52*(5), 1044. https://doi.org/10.1212/WNL.52.5.1044

Rigoux, L., Stephan, K. E., Friston, K. J., & Daunizeau, J. (2014). Bayesian model selection for group studies—Revisited. *NeuroImage, 84*, 971–985. https://doi.org/10.1016/j.neuroimage.2013.08.065

Rossini, P. M., Deuschl, G., Pizzella, V., Tecchio, F., Pasquarelli, A., Feifel, E., Romani, G. L., & Lücking, C. H. (1996). Topography and sources of electromagnetic cerebral responses to electrical and air-puff stimulation of the hand. *Electroencephalography and Clinical Neurophysiology/Evoked Potentials Section, 100*(3), 229–239. https://doi.org/10.1016/0168-5597(95)00275-8

Rossi-Pool, R., Zainos, A., Alvarez, M., Diaz-deLeon, G., & Romo, R. (2021). A continuum of invariant sensory and behavioral-context perceptual coding in secondary somatosensory cortex. Article 1 *Nature Communications, 12*(1). https://doi.org/10.1038/s41467-021-22321-x.

Salti, M., Bar-Haim, Y., & Lamy, D. (2012). The P3 component of the ERP reflects conscious perception, not confidence. *Consciousness and Cognition, 21*(2), 961–968. https://doi.org/10.1016/j.concog.2012.01.012

Schlossmacher, I., Dellert, T., Bruchmann, M., & Straube, T. (2021). Dissociating neural correlates of consciousness and task relevance during auditory processing. *NeuroImage, 228*, Article 117712. https://doi.org/10.1016/j.neuroimage.2020.117712

Schröder, P., Nierhaus, T., & Blankenburg, F. (2021). Dissociating perceptual awareness and postperceptual processing: The P300 is not a reliable marker of somatosensory target detection. *Journal of Neuroscience, 41*(21), 4686–4696. https://doi.org/10.1523/JNEUROSCI.2950-20.2021

Schröder, P., Schmidt, T. T., & Blankenburg, F. (2019). *Neural basis of somatosensory target detection independent of uncertainty, relevance, and reports., eLife*, 8.. https://doi.org/10.7554/eLife.43410

Schubert, R., Blankenburg, F., Lemm, S., Villringer, A., & Curio, G. (2006). Now you feel it—now you don't: ERP correlates of somatosensory awareness. *Psychophysiology, 43*(1), 31–40. https://doi.org/10.1111/j.1469-8986.2006.00379.x

Schubert, R., Ritter, P., Wüstenberg, T., Preuschhof, C., Curio, G., Sommer, W., & Villringer, A. (2008). Spatial attention related SEP amplitude modulations covary with BOLD signal in S1—A simultaneous EEG—fMRI study. *Cerebral Cortex, 18*(11), 2686–2700. https://doi.org/10.1093/cercor/bhn029

Siegel, M., Donner, T. H., & Engel, A. K. (2012). Spectral fingerprints of large-scale neuronal interactions. Article 2 *Nature Reviews Neuroscience, 13*(2). https://doi.org/10.1038/nrn3137.

Soininen, K., & Järvilehto, T. (1983). Somatosensory evoked potentials associated with tactile stimulation at detection threshold in man. *Electroencephalography and Clinical Neurophysiology, 56*(5), 494–500. https://doi.org/10.1016/0013-4694(83)90234-1

Stephan, K. E., Penny, W. D., Daunizeau, J., Moran, R. J., & Friston, K. J. (2009). Bayesian model selection for group studies. *NeuroImage, 46*(4), 1004–1017. https://doi.org/10.1016/j.neuroimage.2009.03.025

Taylor-Clarke, M., Kennett, S., & Haggard, P. (2002). Vision modulates somatosensory cortical processing. *Current Biology, 12*(3), 233–236. https://doi.org/10.1016/S0960-9822(01)00681-9

Torebjörk, H. E., & Ochoa, J. L. (1980). Specific sensations evoked by activity in single identified sensory units in man. *Acta Physiologica Scandinavica, 110*(4), 445–447. https://doi.org/10.1111/j.1748-1716.1980.tb06695.x

Torquati, K., Pizzella, V., Penna, S. D., Franciotti, R., Babiloni, C., Rossini, P. M., & Romani, G. L. (2002). Comparison between SI and SII responses as a function of stimulus intensity. *Neuroreport, 13*(6), 813.

Trajkovic, J., Gregorio, F. D., Thut, G., & Romei, V. (2024). Transcranial magnetic stimulation effects support an oscillatory model of ERP genesis. *Current Biology, 34*(5), 1048–1058.e4. https://doi.org/10.1016/j.cub.2024.01.069

Uemura, J., Hoshino, A., Igarashi, G., Matsui, Y., Chishima, M., & Hoshiyama, M. (2021). Pre-stimulus alpha oscillation and post-stimulus cortical activity differ in localization between consciously perceived and missed near-threshold somatosensory stimuli. *European Journal of Neuroscience, 54*(4), 5518–5530. https://doi.org/10.1111/ejn.15388

Vallbo, Å. B., & Hagbarth, K.-E. (1968). Activity from skin mechanoreceptors recorded percutaneously in awake human subjects. *Experimental Neurology, 21*(3), 270–289. https://doi.org/10.1016/0014-4886(68)90041-1

Vallbo, Å. B., & Johansson, R. S. (1984). Properties of cutaneous mechanoreceptors in the human hand related to touch sensation. *Human Neurobiology, 3*(1), 3–14.

Weisz, N., Wühle, A., Monittola, G., Demarchi, G., Frey, J., Popov, T., & Braun, C. (2014). Prestimulus oscillatory power and connectivity patterns predispose conscious somatosensory perception. *Proceedings of the National Academy of Sciences, 111*(4), E417–E425. https://doi.org/10.1073/pnas.1317267111

Whyte, C. J., Müller, E. J., Aru, J., Larkum, M., John, Y., Munn, B. R., & Shine, J. M. (2025). A burst-dependent thalamocortical substrate for perceptual awareness. *PLOS Computational Biology, 21*(4), Article e1012951. https://doi.org/10.1371/journal.pcbi.1012951

Whyte, C. J., Redinbaugh, M. J., Shine, J. M., & Saalmann, Y. B. (2024). Thalamic contributions to the state and contents of consciousness. *Neuron, 112*(10), 1611–1625. https://doi.org/10.1016/j.neuron.2024.04.019

Wikström, H., Huttunen, J., Korvenoja, A., Virtanen, J., Salonen, O., Aronen, H., & Ilmoniemi, R. J. (1996). Effects of interstimulus interval on somatosensory evoked magnetic fields (SEFs): A hypothesis concerning SEF generation at the primary sensorimotor cortex. *Electroencephalography and Clinical Neurophysiology/Evoked Potentials Section, 100*(6), 479–487. https://doi.org/10.1016/S0168-5597(96)95688-9

Yamauchi, N., Fujitani, Y., & Oikawa, T. (1981). Somatosensory evoked potentials elicited by mechanical and electrical stimulation of each single pain or tactile spot of the skin. *The Tohoku Journal of Experimental Medicine, 133*(1), 81–92. https://doi.org/10.1620/tjem.133.81

Zhang, Y., & Ding, M. (2009). Detection of a weak somatosensory stimulus: role of the prestimulus mu rhythm and its top–down modulation. *Journal of Cognitive Neuroscience, 22*(2), 307–322. https://doi.org/10.1162/jocn.2009.21247

Zopf, R., Giabbiconi, C. M., Gruber, T., & Müller, M. M. (2004). Attentional modulation of the human somatosensory evoked potential in a trial-by-trial spatial cueing and sustained spatial attention task measured with high density 128 channels EEG. *Cognitive Brain Research, 20*(3), 491–509. https://doi.org/10.1016/j.cogbrainres.2004.02.014